CAPITAL UNIVERSITY OF SCIENCE AND TECHNOLOGY, ISLAMABAD

Numerical Study to Enhance the Melting and Solidification of Phase Change Material Using Branched Fins and Nano-Particles

by

Fakhar Ul Hasnain

A thesis submitted in partial fulfillment for the degree of Master of Science in Mechanical Engineering

in the

Faculty of Engineering
Department of Mechanical Engineering

2020

This postulation is dedicated to my parents and teachers, who are constantly a light for me in obscurity and their unflinching help, guided my unfocused words into Sound thoughts

CERTIFICATE OF APPROVAL

Numerical Study to Enhance the Melting and Solidification of Phase Change Material Using Branched Fins and Nano-Particles

by

Fakhar Ul Hasnain

(MME181005)

THESIS EXAMINING COMMITTEE

S. No.	Examiner	Name	Organization
(a)	External Examiner	Dr. Talha Irfan Khan	IST, Islamabad
(b)	Internal Examiner	Dr. Waqas Akbar Lughmani	CUST, Islamabad
(c)	Supervisor	Dr. Muhammad Irfan	CUST, Islamabad

Dr. Muhammad Irfan
Thesis Supervisor
December, 2020

Dr. Muhammad Mahabat Khan
Head
Dept. of Mechanical Engineering
December, 2020

Dr. Imtiaz Ahmad Taj
Dean
Faculty of Engineering
December, 2020

Author's Declaration

I, **Fakhar Ul Hasnain ,** hereby state that my MS thesis titled "**Numerical Study to Enhance the Melting and Solidification of Phase Change Material Using Branched Fins and Nano-Particles**" is my own work and has not been previously submitted by me anywhere else for taking any degree. At any time if my statement is found to be incorrect even after my graduation, the University has the right to withdraw my MS Degree.

Fakhar Ul Hasnain
(MME181005)

Plagiarism Undertaking

I solemnly declare that research work presented in this thesis titled "**Numerical Study to Enhance the Melting and Solidification of Phase Change Material Using Branched Fins and Nano-Particles**" is exclusively my research work with no remarkable contribution from any other individual. Small contribution/help wherever taken has been duly acknowledged and that complete thesis has been written by me.

I understand the zero tolerance policy of the Higher Education Commission and CUST towards plagiarism. Therefore, I as an author of the above titled thesis declare that no part of my thesis has been plagiarized and any material used as reference is properly cited.

I undertake that if I am found guilty of any formal plagiarism in the above titled thesis even after award of MS Degree, the University reserves the right to withdraw/revoke my MS degree and that HEC and the University have the right to publish my name on the HEC/University website on which names of students are placed who submitted plagiarized work.

Fakhar Ul Hasnain
(MME181005)

Acknowledgements

In the Name of Allah, The Most Gracious, The Most Merciful. Praise be to God, the Cherisher and Sustainer of the worlds. All thanks to Almighty Allah, The Lord of all that exist, who bestowed me with His greatest blessing i.e. knowledge and Wisdom to accomplish my task successfully.

Thousands of salutations and benedictions to the Holy prophet **Hazrat Muhammad (PBUH)** the chosen-through by whom grace the sacred Quran was descended from the Most High. I am very thankful to **Dr. Muhammad Irfan**, a great teacher, mentor and supervisor who made a difference in all aspect of my life. I am indebted to **Dr. Muhammad Irfan** for his valuable guidance, encouragement and dedicated support that enabled me to complete my MS Degree Program.

I want to express my heartiest regards to my parents who always supported me morally, spiritually & prayed for my success.

Fakhar Ul Hasnain

(MME181005)

Abstract

In this study branched-fin designs and Nano-particles are used to enhance the melting and solidification process of phase change material (PCM) in a horizontally configured latent heat thermal energy storage (LHTES) unit. Stearic acid is used as PCM whereas water is the heat transfer fluid (HTF). The mathematical model equations are numerically solved for the 2D planar geometries using commercial CFD package ANSYS Fluent. The numerical solution procedure is validated against the results of our experimental setup and the literature. The numerical results show an excellent agreement with the experimental and numerical results of melting fraction, average temperature. A Y-oriented triple-fin design is used as a base case which is the best triple-fin design. The melting phenomena is studied first. Results show a slower melting of PCM in the lower half portion of the unit. This shortcoming is dealt with by proposing five-fin designs with more fins concentrated in the lower portion. Case-1 is an all-straight-fins design. For Case-2 and Case-3, three lower fins are single-branched and double-branched or leaf-vein patterned, respectively. Percentage enhancement ratio and percentage time saving show that Case-3 is the best among the three proposed designs resulting in 1.85 times faster melting as compared to the base case. Analysis of the effects of thermophysical properties of fin and shell materials reveals copper as the best option. The solidification process and the complete melting-solidification cycle is then studied which also reveals Case-3 as the best option. Taking Case-3 as reference case, the effects of Nano-particles concentration on the melting-solidification cycle is finally studied. Al_2O_3 is used as Nano-particles in concentration of 1%, 5% and 10% by volume. Increase in the Nano-particles concentration increases the melting and solidification rates resulting in the percentage time saving of 11.4%, 20.91% and 31.78%, respectively, for the complete melting-solidification cycle. The corresponding energy storage, however, is seen to decrease with an increase in the nanoparticle concentration.

Keywords: Phase Change Material; Branched Fins; Melting; Solidification; Nano-Particles

Contents

List of Figures

List of Tables

Symbols

C_p	Specific Heat, J/kgK
C_{ps}	Solid PCM Specific Heat constant, J/kgK
C_{pl}	Liquid PCM Specific Heat constant, J/kgK
C_{Mushy}	Mushy zone constant
D_t	Tube Diameter, mm
D_s	Shell Diameter, mm
S_t	Shell Thickness, mm
L_s	Side Length, mm
g	Gravity, m/s^2
h	Enthalpy, J/kg
k_{PCM}	Thermal Conductivity of PCM, W/mK
l_f	Fin Length, mm
L_f	latent Heat of Fusion, kJ/kg
Nu	Nusselt number
$\overline{Nu}$	Average Nusselt number
Q_{stored}	Total Energy Storage, W
Ra	Rayleigh number
Ste	Stefan number
t_t	Inner tube Thickness, mm
t	time, min
$t_{M,max}$	Maximum Melting time, min
$t_{M,min}$	Minimum Melting time, min
t_M	Melting time, min

t_f	Fin Thickness, mm
T	Temperature, K
T_s	Solidus Temperature, K
T_l	Liquidus Temperature, K
T_R	Reference Temperature, K
T_{HTF}	Heat transfer fluid temperature, K
T_{PCM}	PCM temperature, K
u_i	Velocity component, m/s
$\overline{\alpha_1}(t)$	Melting fraction of case 1
$\overline{\alpha_i}(t)$	Melting fraction of any case
ρ_l	Liquidus density, kg/m^3
ρ	Mean density, kg/m^3
ρ_s	Solidus density, kg/m^3
μ	Viscosity, kg/ms
ϵ	Small number
s	Solidus
t	Tube
l	Liquidus
c	Coefficient
f	Fin
r	Ratio
R	Reference
th	Thermal
M, max	Maximum Melting
M	Melting
M, min	Minimum Melting

Abbreviations

CFD	Computational Fluid Dynamics
HTF	Heat Transfer Fluid
LHTES	Latent Heat Thermal Energy Storage
LG	Liquid Gas
MUSCL	Monotone Upstream-Centered Scheme for Conservation Laws
NEPCM	Nano-Particals Enhanced Phase Change Material
NP	Nano-Partical
PCM	Phase Change Material
PRESTO	Pressure Staggering Option
PISO	(Pressure Implicit with Splitting of Operator
SL	Solid Liquid
SIMPLE	Semi-Implicit Method for Pressure Linked Equation
SG	Solid Gas
SS	Solid Solid

Chapter 1

Introduction

1.1 Background

The sustainable development of the modern world is based on the energy resources and their purposeful utilization. The major chunk of the present-day energy comes from the fossil fuels. Due to the depletion of the current fossil fuel reservoirs and because of their negative impact on the environment, there is always a quest for the efficient, clean and reliable energy sources. Renewable energy sources are, of course, strong candidates because of being environment friendly but they lack in their continuous availability. A possible solution to such a situation can be to store the energy when it is available and use it when desired, i.e., energy storage systems. Different energy storage systems are in practice to store and retrieve different types of energies, e.g., flywheels to store mechanical energy, batteries to store electrochemical energy, biofuels to store chemical energies, thermal energy storages to store thermal energy, etc. Classification of different thermal energy storage system are shown in **Figure: 1.1**. Thermal energy storage systems are cost efficient, reduce greenhouse gas emissions and a promising step towards less carbon future. They also improve the performance, authenticity and reliability on Energy storage systems. Some types of LHTES system have been shown in **Figure: 1.1**. Development of LHTES system has received a lot of attention

for the past two decades because of its ability to store thermal energy efficiently. Different techniques are used these days to store thermal energy. Thermal energy storage is the storage of energy at very low or high temperature, to use it later. Simplest of all is using sunlight to store energy in the day time and using it later in the night. A typical charging-discharging process includes charging the system when energy is readily available and using it when needed. This process is concurrent, and the system repeatedly acts the same way. LHTES system is measured a significant technology that allows a lasting use of renewable energy systems.

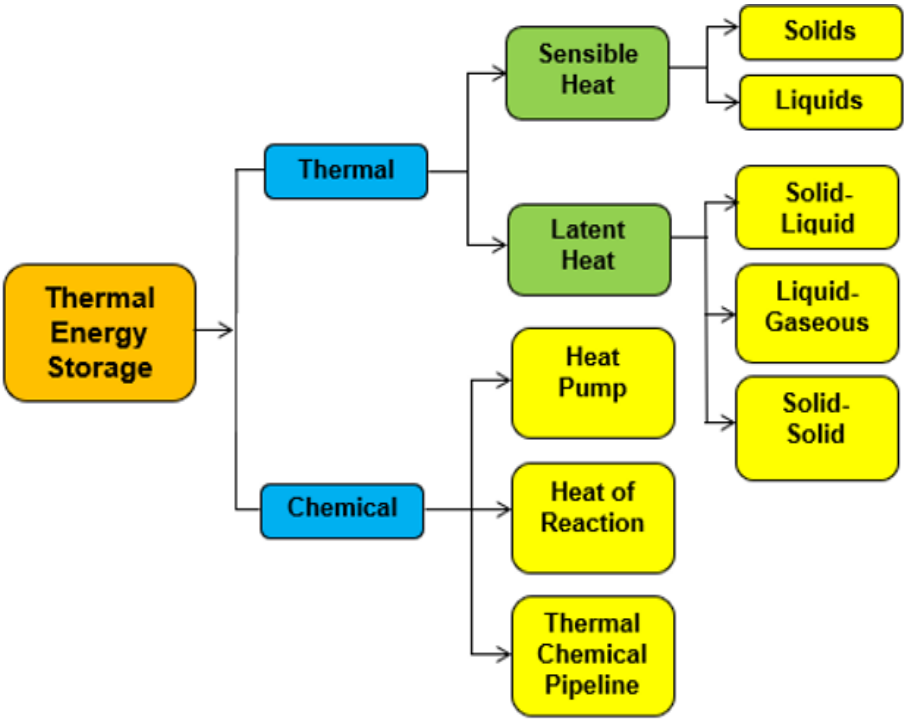

FIGURE 1.1: Types of Thermal Energy Storages (Kadivar et.al., [1])

1.2 Thermal Energy Storage

Nikolay et.al [2] studied different sustainable energy sources. Mainly there are three main types of thermal energy storage systems which includes:

- Sensible heat storage systems
- Latent heat storage systems
- Thermochemical storage systems

1.2.1 Latent Heat Thermal Storage Systems

Latent heat storage thermal energy storage (LHTES system) uses phase transition phenomenon for the extraction of energy. Most commonly solid to liquid phase transition is possible for the energy extraction. Solidification and melting are two common processes involved in the LHTES system. In melting process heat is transferred and stored in the material and later in solidification this heat releases and respective amount of energy is obtained. PCMs are the materials which are used in LHTES system. Due to non-toxic, non- poisonous behavior of PCMs, LHTES system are considered as one of the environment friendly thermal storage systems. Moreover, they have higher energy density they require less volume as compare to sensible storage systems.

Initially, LHTES system stores sensible heat but once the phase change temperature is achieved, PCM temperature remains fixed while phase change takes place and latent heat is stored. Solidification process is the reverse process in which the PCM discharges heat and again changes the phase. **Figure: 1.2** shows the change in enthalpies of a storage medium while charging and discharging.

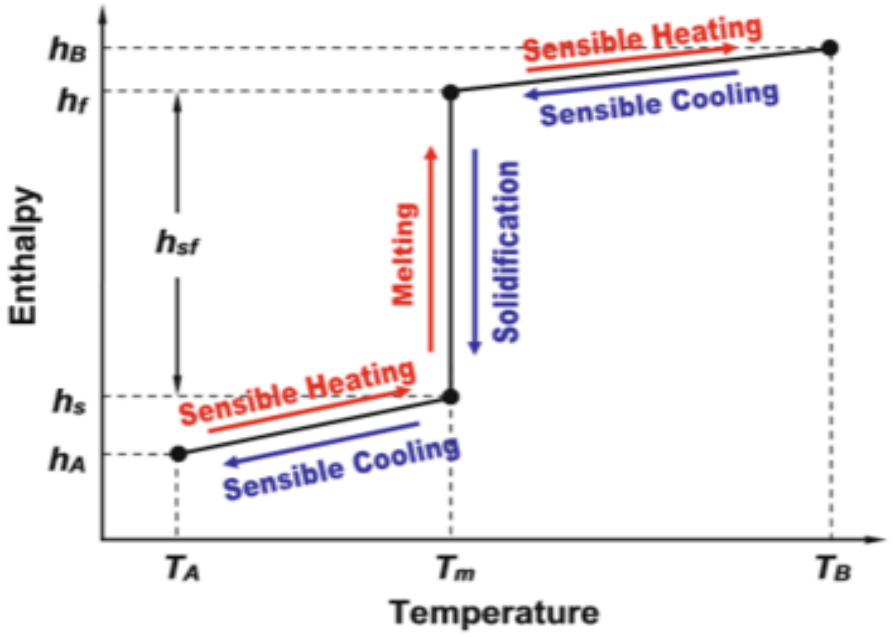

FIGURE 1.2: Variations In Enthalpies During Heating And Cooling Process(Anon et.al., [4])

1.2.2 Types of Phase Change

Following forms of phase transitional systems can be studied:

• **SL**: A system that changes phase from solid to liquid or vice versa upon heating or cooling respectively.

• **SG**: A system that involves phase change between solid and gas states.

• **LG**: In this system transition take place from liquid to gas during phase change process.

Solid -Liquid systems is preferred over the other because in this phase change system the operating pressure is lower than any other system [4].

Following are the key components of a LHTES system unit:

1.2.3 Phase Change Material (PCM)

Phase change material is storage medium that endures a phase transformation when it meets the transition temperature. Phase change material must be selected according to its transition temperature and the temperature requirement of application.

1.2.4 Heat Transfer Fluid (HTF)

Heat transfer fluid is the medium that transfers energy from source to PCM and vice versa. Operating conditions of HTF greatly influence the working of LHTES system. Water is usually the first choice of HTF

1.2.5 PCM Properties

PCMs should satisfy following properties for practical applications.

- PCMs should have suitable melting point that is easily attainable without any special energy requirements.

- PCMs should possess high phase change enthalpy.
- PCM specific heat capacity should be high.
- It is also required for PCM to have high thermal conductivity.
- Density of the PCMs should high as well.
- PCMs with the low volumetric strain and low vapor pressure are preferred.
- PCMs should not have phase separation.
- PCMs should be non- toxic, non-corrosive, inflammable and environment friendly.
- PCMs should have reversible phase transition.

1.2.6 Solid-Liquid Phase Change Materials

Phase change Material used in LHTES system can be categorized into following types:

- Organic
- Inorganic
- Eutectic

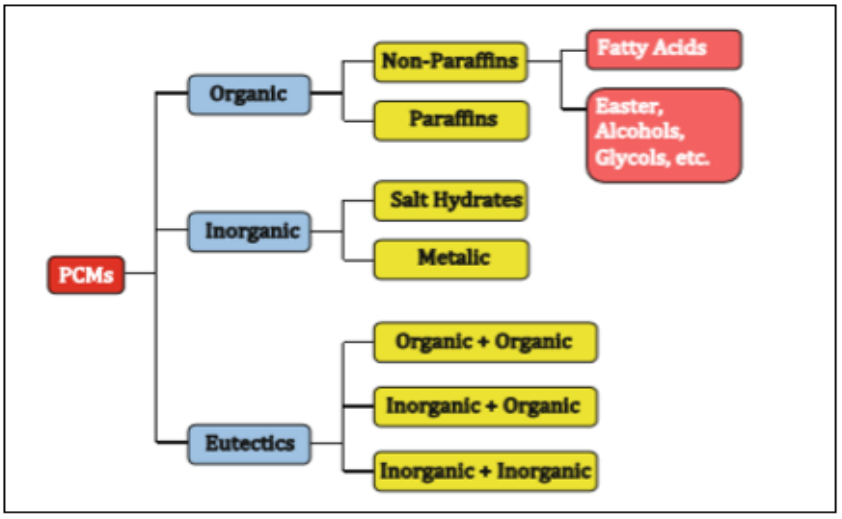

FIGURE 1.3: Classification of PCMs [6]

1.2.7 Organic PCM

Organic materials have outstanding thermal properties. The melting is congruent and Phase change temperature range is narrow. They exhibit self-nucleation and high density. Most of the organic materials do not display phase segregation and low supper cooling [6]. These types PCMs are suitable for conservation of energy in buildings, development of solar energy units, keeping batteries and electronic devices cool and textile industries.

1.2.8 Inorganic PCM

Inorganic materials have higher thermal conductivity. These materials are usually low cost and their latent heat capacity is higher than organic material.

1.2.9 Eutectic Mixture

Eutectic mixtures give the opportunity to adjust phase change temperatures. These materials do not segregate during melting and freezing. Moreover, mixture of molten salts could reduce the melting point. PCMs can be used in a variety of applications but the main concern is regarding the selection of the PCMs. PCMs for different applications are selected on the bases of different properties including thermal properties, physical properties, kinetic properties, chemical properties, and economic feasibility [6]. Stearic acid is selected as steric acid losses its sensible heat very fast but takes a long time to release its latent heat which makes it a perfect material for LHTES system applications.

1.2.10 Limitations of LHTES System- A Research Avenue

Phase separation, supercooling, liquid leakage and low thermal conductivity are most common problems of PCM. But most of the PCMs suffer from lower thermal

conductivity which makes heat transport with in the PCM a challenging task.
There are different methods for heat transfer improvement. The objective of these method is to enhance thermal conductivity of PCM to improve the transfer of heat. This impact the phase process and improves overall performance. One way to enhance thermal conductivity with high conductivity materials such as metals, metallic oxide nanoparticles and carbon materials.
Another way of enhancing the PCMs heat transfer through increasing natural convection of liquid PCM. Commonly used LHSUs are tube -in-shell, triplex-tube and rectangular. Fin of different shapes like rectangular, cylindrical, spherical and annular are commonly used to improve the thermal conductivity [7]. Thermal conductivity can also be improved by addition of nanoparticles having nominal magnitudes ranging from 1-100mm. [8]
Sarbu and Dorca [9] studied several methods for thermal storage units to enhance heat transfer. These methods can be generally classified into following categories:

- Using High conductive materials(nanoparticles)
- Using additional materials
- Encapsulation method
- Using fins
- Shell geometry optimization
- Tube geometry optimization
- Heat pipes
- Cascaded storage

1.3 Scope and Objective of this Work

The currrent study attempts to resolve the low thermal conductivity issues by introducing innovative fin design and addition of nan-particals are proposed by straight, single branched and double branched or leaf-vein patterned fin designs for the melting and solidification enhancement of Phase change materials using horizontal LHTES system unit. Although the advanced manufacturing technologies available today allow designers to go for the more complicated fin designs but

nothing is better than the simpler fin shapes [10]. Stearic acid is used as PCM for the current study while water serves as HTF. Transient numerical simulations are performed to examine the melting and solidification performance of PCM in 2D planar configurations using commercial solver ANSYS Fluent. Mathematical results are first associated with the present investigational results and those from the literature to validate the mathematical model used and the numerical solution strategy employed. The new fin designs are proposed by analyzing the weaknesses of the Y-oriented triple-fin design which is the best among all possible orientations of the three fins design and is selected as base case for our study. All new proposed designs have five fins each. Case-1 is an all-straight-fin design. In both Case-2 and Case-3, three lower fins are singly-branched and doubly-branched or leaf-vein patterned, respectively. Additional fins and branches are adjusted by reducing the thicknesses of the fins and branches such that the systems contain same amount of PCM for all the cases. The performance of the new fin designs is gauged by analyzing the melting and solidification time, average temperatures of PCM, total heat storage, storage rates, percentage time saving and enhancement ratios. The effects of the thermophysical properties of fin and shell material are also analyzed by simulating several case studies with different fin and shell materials. Furthermore, the properties of the heat transfer fluid temperature are also analyzed by simulating various Stefan number cases and monitoring the melting times and average Nusselt numbers.

To improve melting and solidification processes and to decrease melting and solidification times, effects of geometrical properties are explored in this study. Effects of nano-PCM on melting and solidification time is also investigated using different percentage of aluminum oxide as a nano-PCM. First, melting performance of the most efficient fin design is further enhanced and investigated by adding nanoparticles into the PCM. The results are discussed and compared based on enhancement ratio and time saving. it is observed that adding aluminum oxide improves the melting time. Then average energy storage and energy storage rate is also discussed it is observed that by adding aluminum oxide the latent heat decreases and hence it leads to decrease in the energy storage rate. The melting

performance indicators and energy storage capacities are analyzed for various concentrations of nanoparticles for the melting and solidification complete cycle. It is observed that the addition of nanoparticles is also significant in complete melting and solidification cycle.

1.4 Thesis Overview

Chapter 2 is about literature survey regarding phase change materials. In this chapter relevant work regarding problem at hand will be discussed. A detailed literature review will be carried about heat transfer augmentation techniques and methods involving phase change materials.

Chapter 3 is related to numerical setup of simulation used for studying phase change process of thermal energy storage unit. It consists of problem statement and analysis domain and geometry. It also includes meshing strategy, boundary conditions, governing equations and Ansys fluent setup for simulations.

Chapter 4 presents the results obtained from this numerical study. The results section is mainly divided into two sections. First section includes the configurations and different arrangements of LTESU for melting and solidification process. Whereas, the second section discusses the results obtained by optimizing with adding nano-particles in base PCM, using best fins configurations.

Chapter 5 consists of conclusions of this research study. This chapter also consists of the future recommendations in the area of study under consideration in this work.

Chapter 2

Literature Review

Latent heat thermal energy storage (LHTES) systems offer several advantages over their counterparts [11]: (1) To store the same amount of energy LHTES system needs less weight and volume of the material, i.e., more energy density (2) it stores energy nearly at constant temperature, i.e., the phase change temperature of the PCM. Variety of PCMs are now available with a wide range of melting temperatures. Phase change material selected for a specific application should melt within desired temperature range of application. Researchers have predominantly focused the application areas in the temperature range of 0–65 °C which involves domestic heating/cooling [13], [14], cooling of electronic devices [15], [16], thermal storage of solar energy, refrigeration applications [17]–[18] , etc. Several designs of the LHTES systems are studied by the researchers based on the design requirements. These include cylindrical shell and tube units installed horizontally or vertically and the rectangular or slab type systems. The simplest one is the concentric shell and tube heat exchanger configured horizontally because of its better thermal performance as compared to the vertical one [19].

The PCM is filled in the gap between the outer shell and the inner tube. The heat transfer fluid (HTF) flows over the inner tube and melts the PCM: the process called charging; and reverse process is called discharging in which the PCM solidifies. The melted PCM rises upwards due to buoyancy creating convective currents that accelerates the PCM melting on the upfront. But in the lower half section of

the container PCM melts very slowly because of the extremely low thermal conductivities of almost all the PCMs: a grave disadvantage. Therefore, it takes longer time to completely melt the PCM in the system and questions the effectiveness of the latent heat thermal energy storage systems. To resolve this issue different techniques have been proposed and tested by the researchers with an ultimate objective of improving the heat transfer between the HTF and the PCM during charging and the discharging processes. These include the tubes with variety of fin configurations [20]–[22], using nanoparticles [23], [24], metal foams [25]–[27], highly conductive particles in the PCM [28], using multi tubes heat exchanger [29]–[31] and the micro-encapsulation of the PCM [32]–[34]. Finned tube is the most widely studied strategy for enhancement of the heat transfer due to its simplicity and durability, ease of manufacturing and installation and excellent heat transfer improvement characteristics. Fins attached to the HTF tube on one side and embedded into the PCM on the other side effectively transport heat between the HTF and the PCM by increasing the heat transfer area.

Abhat et al.[35] performed an experimental study to examine the performance of a shell-and-tube heat exchanger with three different PCMs: paraffin, fatty acid and salt hydrate with melting point in the range of 20–80 C. A finned-annulus heat exchanger element with aluminum fins radially located was used as the PCM container. Results indicates a substantial effect of thermal cycling and natural convection on the melting and solidification performance of the storage materials.

Gharebaghi and Sezai[36] studied numerically the rectangular arrangement through adding of straight fins to the plumb intense walls for the heat-transfer improvement. Individually the intense walls were preserved at a fixed temperature that was more than the PCM melting point. Installation of perpendicular heated walls with straight fins were much favored since enhancing temperature transmission rate, related to straight intense walls with perpendicular fins.

Vogel et al.[37] found that the effect of natural convection rises with larger continuous areas of storage material, larger tube spacing and smaller fin volume fraction in vertical finned tube LHTES. Hence, reduction of heat transfer rate with compact amount of fin material is partially compensated. Secondly, large fin heights

lead to reduction of improvement of temperature transmission by natural convection. Choi and Kim et al. [38] experimentally improved the heat-transfer rate through circular fins to phase change material during discharging process in tubular arrangements joined to circular fins. The temperature rise by entirely circular positions were higher intended for a finned arrangement, as compared to without fins.

Pascal et al. [39] numerically investigated the effect of fin size and distribution on solid-liquid phase change for a rectangular enclosure. They investigated that with increase in number of fins stabilization temperature reduces and it increases the sensible and latent energy storage of the PCM. Hosseini et.al., [40] performed experimental and numerical investigation to study the effect of fin length and Stefan number on the performance of LHTES. Analysis was performed for three different lengths and Stefan number. It was concluded in their work that 26mm fin length and 0.38 Stefan number enhanced melting process and increased system performance by 15.3%. Kamkari et al. [41] studied the experimental investigation of the melting of Lauric acid (PCM) in the quadrangular enclosure with horizontal partial fins. By increasing number of fins, the melting time decrease and results in an improvement in the overall heat transfer rate. Yagci et al. [42] experimentally studied performance optimization of vertical LTESS through longitudinal fins. Commercial grade paraffin was placed between annular gap and fins with different length-edge ratios were installed. Comparing melting and solidification time with non-finned LTESS, 62% and 58% improvement was achieved respectively.

Castell et al.[43] used perpendicular peripheral longitudinal fins throughout discharging method for LHTES unit. Temperature transmission augmentation remained effectively attained through the perpendicular longitudinal fins on the tube adjacent effectively endorse natural convection. But, once the temperature transmission factor found, the discharging period remained still not as much since the increase in the temperature transmission region. Mosaffa et al. [44] presented a estimated systematic model for cooling systems. Phase change material stood solidified in the tubular shell, by way of dissolute in a quadrilateral stowage taking the equal capacity and temperature transmission zone. The compact segment

of the phase change material similarly growths rapidly, once cell aspect ratio get smaller.

Solomon and Velraj[45] by experimentation work estimated phase change material applied for the refrigeration structure through apparent tubular discharging using the dual pipe heat exchanger. Phase change material occupied in the ring lengthwise eight perpendicular frequently spread out copper fins of changed elevations then air heat transfer fluid fleeting over the internal tube. Total discharging period was reduced due to the refrigeration amount improvement by perpendicular fins. Furthermore, maximum materials of fins selected copper to intensification the temperature transmission rate and arrangement of fins used internal and external fins developed inner side to the PCM vessel.

Ermis et al.,[46] used a procedure intended for thermal examination of the change of phase in storage unit through the spherical finned tube. The temperature storing over phase change material near regions to tube also empirically examined. The writers concerned about impact of the extended surfaces and parameter of flow through explaining the main equations of heat transfer fluid, wall of the pipe, and phase change material. Accumulation of spherical fins to the Latent heat thermal energy storage unit enlarged temperature transmission rate and improved the rate of mass fraction throughout the charging and discharging process.

Ismail et al. [47] statistically and experimentally considered the solidification behavior of PCM around a vertically axially finned isothermal cylinder. It was observed that fin thickness has a minor effect on solidification while fin length, the aspect ratio of annular fins, and the number of fins have a strong influence on the solidification. It was observed that four to five fins of equal thickness and having length equal to twice the diameter of a tube was considered as an optimum case. Literature reports several studies exploring the effects of different fin parameters including their material, shape, design, orientation, length, thickness, number of fins and their annular arrangement around the tube on the heat transfer improvement. The shape and design of the fin is an important parameter for heat transfer enhancement and several studies reveal innovative find designs in this regard.

Velraj et al. [48] worked on mathematical and investigational methods intended

for a thermal stowage expedient containing perpendicular spherical tube finned on internal surface, and occupied by paraffin RT60. Given setup positioned inside alternative spherical tube comprising water as a HTF. Outcomes presented that the V shaped arrangement were highest beneficial in term of energy storage. It is also found that total discharging period for V shaped arrangement around abridged to (1/n) related it to without fins geometry (where n= number of fins).

Rathod and Banerjee et al. [49] examine a perpendicular shell and tube by means of three perpendicular fins arranged on internal tube to examine the improved charging and discharging process of paraffin PCM. Results indicates that 25% saving in charging period while 44% saving in discharging period by fins addition. Investigation of outcomes revealed that temperature transmission growth owing to fins addition is further delicate toward the rise in the heat transfer temperature as compared to the rise in the heat transfer fluid flow rate.

Sciacovelli et al. [50] worked on numerical study for improving the performance fins of Y arrangement with divisions having the arrangement of three arrangement, having shape of snow flake and ring arrangement fins. Outcomes of study presented that the effectiveness of energy retrieval enlarged up to 24% after optimum fins when dual branching is used. Investigation for the optimizing results showed that here a relationship occurs among the extent of working time and optimal fin geometry. It is also observed fins of Y shaped with different angles among divisions are favored for small working periods while fins with slighter angles are favored for large working periods.

Eslami et al .[51] worked on sensible and latent thermal energy storage tank. Three different fin geometries with optimum dimensions are considered. The more complex fin arrangement like V and pencil shaped design attain a more uniform melting and solidification behavior in sensible thermal energy storage.

Park et al[52]., experimentally study natural convection from vertical cylinders with branched plate fins for solidification. Several branch angles, number of fins, and base temperatures are observed. Comparison the thermal resistances of cylinders with branched fins and conventional plate fins and find that cylinders with branched fins show thermal resistances up to 36% lesser than cylinders plate fins

resistances. Xie et al.[53] worked on transient mathematical prototypical based arranged the Capacity of Liquid then enthalpy porosity technique to examine the active thermal performances of phase change material inclusions.

The outcomes presented that enhanced branched form arrangements through improved temperature dispersion effectiveness attained improved temperature homogeneity in the phase change material inclusion by way of their complements in the plate fin temperature sink arrangements. A advanced metallic capacity fraction remained satisfactory intended for a improved temperature consistency in the phase change material inclusion and later gained a lesser heat font temperature owing to the better complete thermal conduction of phase change material inclusion.

Sheikholeslami et al. [54] studied the discharging/solidification process of LHTES system in a perpendicular square shell using snowflake crystal like fin configuration. It resulted in 2.0 times faster solidification in comparison with the simple longitudinal fin system. Pizzolato et al. [55], [56] developed an algorithm that designs the optimal fin shapes using topology optimization and computational fluid dynamics for efficiently storing and subsequently delivering the desired amount of energy under time constraints. Their study also revealed that optimum melting and solidification demand for fundamentally different fin layouts. Luo and Liao [57] used current framework Boltzmann method for simulating the melting process of the PCM in a opening occupied with tree-designed fins. A study revealed that increasing the number of branching levels resulted in faster melting. Furthermore, selection of suitable bifurcation angle results in more efficient heat transfer performance. Zheng et al. [58] numerically studied different types of tree-designed fins to enhance the solidification of the PCM and identified a particular design which resulted faster as well as uniform solidification. Zhao et al. [59] used topology optimization method to design different fin configurations for the LHTES system. Their optimum fin design enhanced the heat transfer such that the melting and solidification time is reduced by 70 % and 81 % correspondingly as compared to a reference straight 4-fin design. Liu et al. [60] proposed an innovative longitudinal triangular fin to enhance the solidification process and got a 38.3 % decrease in the solidification time as compared to reference traditional rectangular fin.

Highly Conductive nanoparticles when mixed with PCM increases thermal conductivity of the mixture and therefore accelerate the melting and solidification process. Literature reports various nano particles being used in different concentrations with a variety of PCMs to analyze their impact on thermal properties and performance of LHTES system.

Elbahjaoui et al.[61] found that diffusion of high conductivity nanoparticles accelerate the storage performance of pure PCM and enhance the solidification rate. In addition, the high distribution of nanoparticles $\phi \leq\%$) allows the discharging of the large total latent heat from NEPCM in a shorter time.

Khodadadi et al. [62] analytically find that the dispersion of nanoparticle in the phase change material enhanced the effect of thermal conductivity. Alizadeh et al. [63] inspected the thermal efficiency of latent heat stowage system using V-shaped fins and nano-PCM. They illustrated that nano-PCM improves the solidification time 1.49 times and 1.16 times using 2.5% and 5% nano-PCM respectively. Dislva et al. [64] study the effects of nanoparticles numerically and experimentally in solar still applications. They found experimentally that there is a 35% improvement in total discharging time with the nanoparticle. Kalaiselvam et al. [65] analytically and experimentally investigate nanoparticle-PCM intended for refrigeration application in building materials. From the Experimental results, they find out that solidification time is reduced by using nanoparticle embedded phase change material. The solidification time for the 60% n-tetradecane: 40% n-hexadecane PCM embedded with the aluminum and alumina nanoparticles decrease 12.97% and 4.97% correspondingly. In addition, the test results designate that with increasing the mass fraction of the nanoparticles greater than 0.07 the rate of solidification was not significant.

Parsazadeh and Duan [66] studied PCM charging process using shell and tube heat exchanger in the existence of extended surfaces fins and nanomaterials. Outcomes indicated that the improved result of nanomaterials differs for changed fin geometric constraints. The charging time intensifications up to 6% from actual charging time at optimum fin angle of 35 degree and 4% for aluminum oxide nanomaterial. Lohrasbi et al.[67] studied solidification procedure using latent heat

storage system in the existence of fins and nanomaterials. The fin of V arrangement endured involved to the Heat transfer fluid to transference temperature to the phase change material. Properties for geometric constraints for current fin arrangement considered. Outcomes of the study showed that adding nanomaterials improves thermal conduction of the phase change material hence, improves the process of phase transformation, dipping fins for appropriate arrangement inside phase change material attains suggestively high phase transformation rates.

Mahdi and Nsofor et al.[68] described a numerical study of charging process for triple tube temperature exchanger advancing as of extended surfaces fins and nanomaterials. Influence of extended surfaces sizes and nanomaterials capacity on the growth of the mushy zone, dispersal of warm front, and chronological shape of molten fraction throughout charging process examined. Outcomes indicated that retaining the amalgamation of extended surfaces fins and nanomaterials is effective instead of using nanomaterials alone.

It is also observed that rise of heat transfer fluid temperature pays to phase change material charging period enhancement. It also improves the probable of nanomaterials and fins collective effects. Lohrasbi et al.[69] examined the outcome of extended surfaces fins with distinct divisions exclusive the stowing system comprising phase change material and associated the arrangement of system in the existence of the advanced shaped fin and Cooper oxide nanoparticles. Outcomes showed by means of the advanced shaped novel fins arrangement effectively improves solidification time.

Results also showed that present improvement is greater related to arrangement in the existence of Cu oxide nanomaterial. Outcomes showed that existence of extended surfaces fins ensures not face convention restrictions together with viscosity rise and unwanted deviations of properties. Results indicated that by adding 2.5 and 5% volume fraction of copper oxide the solidification rate is increased by 1.099 and 1.208 respectively. Darzi et al. [70] considered charging and discharging of phase change material using fins and nanomaterials in tubular annulus through constraints consisting outline of the storing component, quantity of arranged fins and capacity of nanomaterials. Results indicated that diffusing nanomaterials in

the phase change material increases charging and discharging process, Conversely, using fins origins substantial improvement of the charging and discharging process. That's further effectual through the discharging for conquest of the usual convection tornados in charging . Their results showed that V shaped fin, radial fins and simple longitudinal fins improve the discharging rate by 4.214, 3.58 and 3.30 times as compared to without fins heat pipe.

Mahdi et al. [71] providing a complete analytical study of triplex-tube LHSS proceeding from the collective use of nanoparticles and fins. The complete solidification time can be reduced efficiently with the dispersal of nanoparticles. The small magnitude of nanoparticle spread in the base PCM increases transport of energy. Micro convection properties are influenced in the nanoparticle PCM that improve melting and solidification time. They used up to 0.02 volume fraction and reduction in total solidification time is about 59% at 363K by rising HTF temperature up to 373K this enhancement in total solidification time reached about 60.5%.

Sheikholeslami et al. [72]worked on an advanced fin arrangement, based on snowflake crystal construction. The efficiency of nanomaterials dispersal in phase change material and accumulation fin with changed constructions on LHTES performance have been inspected. Outcomes indicate that attaching fins is a good enhancement technique for discharging process in LHTESS in comparison with nanoparticle dispersion By using Snowflake shaped fin in LHTES, discharging process completes approximately 8.3 and 2.0 times faster in comparison with LHTESS without fin and with simple longitudinal fin respectively.

Darzi et al. [73] numerically examined charging and discharging process for three of different orientation of cylinder annulus by using extended surfaces fins and nanomaterials. The charging period decrease 39%,73%,78% and 82% by using 4,10,15 and 20 longitudinal fins respectively. It was also observed that discharging period is decreased by 28%,62%,75% and 85 % by using 4,10,15 and 20 fins respectively. The discharging period is reduced by 9% and 16% by using 2% and 4% nano particles in the base PCM.

Abduleef et al. [74] numerically examined LHTES by means of triplex tube heat

exchanger with longitudinal fins and outcome of dispersal of nanomaterials. They examined internal, internal-external and external fins. Their outcomes showed that by adding 10% Alumina in base PCM improve thermal conductivity up to 25%. This increase in thermal conductivity leads to decrease in total charging period 12%, 11% and 17% for three proposed designs of fins respectively. They also detected that thermal performance of external fins by means of nano PCM is improved 14% and 11% associated to internal and internal -external fins.

Arici et al. [75] numerically inspected the charging process in a square inclusion by means of internal fins and nanomaterials. Copper oxide is used as nano-particle. charging time is reduced from 27 to 52% depending upon length of fins and 13 to 68% depending upon the orientation of fins. By inserting nanoparticles shorter fins give the higher thermal performance equivalent to long length fins without inserting nanoparticles in the base PCM.

Xiong et al. [76] reviewed all the nanoparticles studies where they reached on conclusion that diffusion of high conductive nano structure was very effective method to advance thermal performance of PCMs. The effects of nanoparticles are mostly engrossed on charging and discharging inside different container with quadrilateral cavities, tubes, cylinder etc. The key results of this study are that nanopcm is more operative in discharging process as related to charging.

Sheikholeslami et al. [77] reviewed on the methods of accelerating thermal performance of LHTES. They find that about 54% articles used paraffin as PCM. Shell and tube configurations are used by 21.54% researchers among other configurations while 51.5% papers focused on the using longitudinal fins as compared to other fins design and 31% researchers focused on used nano-PCM to improve thermal performance as compared to other techniques. Arasu et al. [78] perform numerical investigation in concentrical dual pipe heat exchanger. They enhanced thermal performance by introducing alumina as a nanoparticle in paraffin wax. Their outcomes showed that 23KJ, 20KJ and 29KJ more energy storage and 28KJ, 35KJ and 46KJ more energy retrieval using 2%, 5% and 10% alumina nanoparticles.

Babzadeh et al. [79] numerically replicated heat release system using finite element method. They examined different percentage and different size of diameter

of nanoparticles. The best value of diameter of nano particle to improve the extreme discharging rate at 40nm.

Hung et al. [80] studied discharging process inside a tank with spherical and wavy cold sides. To improve the thermal performance of copper oxide nano powder with changed diameter utilized. Their outcomes showed that discharging period reduces 19.89% and 18.85% with nanoparticles diameter size of 30nm and 40nm.

Hossenzadeh et al;[81] numerically worked on triplex container using rectangular fins to enhance solidification rate. Their results showed that by addition of fins to LHTES 8% increment in the discharging rate. The total discharging time is reduced 12% by applying hybrid nano particles and fins. Lamina shaped hybrid nano particles enlarged 4% discharging rate.

Hajzadeh et al. [82] analyzed the effectiveness of discharging unit by means of fins and nano particles. Copper oxide is used as nano-particle while RT35 was base PCM. Three different designs with one without fins and two with alternate arrangement of Y-shaped fins was investigated. The discharging period for the two Y-shaped designs with nano-PCM reduced 70.66% and 69.2% respectively as compared to without fins.

Fanghua et al;[83] numerically examined the extended surfaces and nanoparticles to increase discharging rate within chamber equipped with fins. Their results showed that highest effect of length of fin occur when sphere nano powder exists and 27.37% reduction in discharging about 1.12 times then by inserting 0.04 mass fraction of nanoparticles.

Hossenzadeh et al. [84] performed finite element method investigation to study the hybrid nano enhance phase change material in LHTES in the existence of tree structured fins. The key result of the study was that by introducing hybrid nano particles in base PCM the dispersion depth increase that leads to reduction in total solidification time.

Sheikholeslami et al. [85] numerically study combine effect of nano particles and fins in the existence of radiative temperature transmission. Copper oxide was selected as nano particle. Outcomes of this study showed that by means of longer fins and inserting nano particles improve discharging rate.

All the above researches laid the foundation for this study. We obtained different points from all these studies and observed the shortcomings of their work. In the same way, the current study is aimed to inspect the charging and discharging process of different design of fins and using nanoparticle inside the PCM in a latent heat storage system. The time of absorption of heat in the latent heat storage system is reduced by accelerating the melting process and the total time spent on transferring absorb heat to the ambient is reduces by accelerating the solidification process.

Chapter 3

Problem Formulation

3.1 System Design and Thermo-Physical Properties

A horizontal configuration of the cylindrical shaped concentric shell and tube type LHTES system is studied numerically to explore the heat transfer enhancement between the HTF and the PCM during the melting/charging and solidification/discharging operation using several fin designs and configurations. A triple-fin Y-shaped LHTES unit is considered as the base case for this study because of its best melting performance among all the orientations of triple-fin design [10]. The schematic of the base case is shown in **Figure: 3.1**. The inner diameters of the shell 'D_s' and tube 'D_t' remain constant throughout the whole study and are 121 mm and 32 mm, respectively, and the corresponding thicknesses, 't_t' and 't_t', are 3 mm each [10]. The radial length 'l_f' and thickness 't_f' of each fin is 36 mm and 3 mm, respectively. Three fins are 120° apart from each other. The HTF flows through the pipe on which fins are installed whereas PCM fills the space between the shell and the tube such that the fins are embedded in the PCM. The material for the outer shell is steel whereas tube and fins are made of copper.

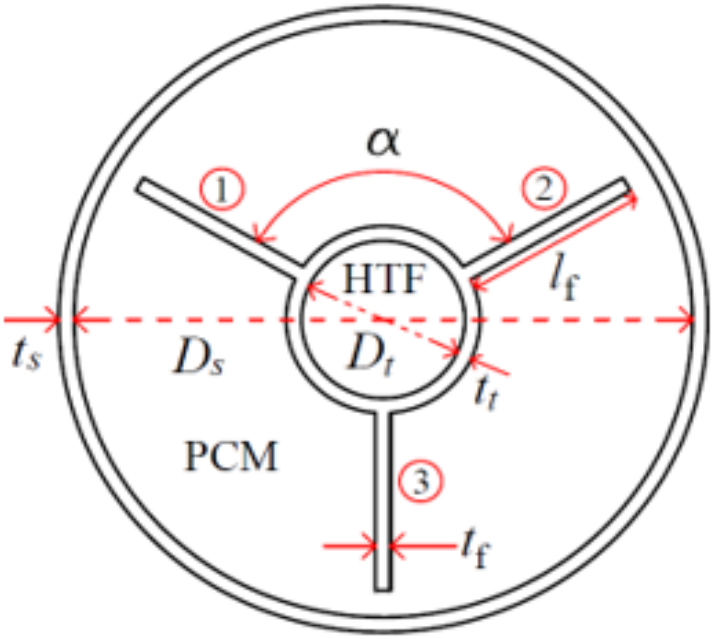

FIGURE 3.1: Schematic Representation of the Y-Oriented Triple-Fin Base Case Design

Stearic acid is used as PCM because of its lower melting temperature, good physical and chemical properties such as non-toxicity and non-corrosiveness. Thermophysical properties of Stearic acid are listed in **Table: 3.1**, whereas, the properties of steel and copper are given in **Table: 4.1**.

TABLE 3.1: Thermophysical Properties of the Stearic Acid Used as PCM [10]

Properties	**Stearic Acid**
Liquidus Temperature of PCM, Tl (K)	337
Solidus Temperature of PCM, Ts (K)	327
Dynamic Viscosity, μ (kg/m-s)	0.0078
Specific heat of PCM, solid, Cps (J/kg-K)	2830
Density of PCM, solid, ρ_s (kg/m3)	1150
Density of PCM, liquid, ρ_l (kg/m3)	1008
Specific heat of PCM, liquid, Cpl (J/kg-K)	2380
Thermal Conductivity, k (W/m-K)	0.18
Latent heat of fusion, Lf (kJ/kg)	186.5
Thermal expansion coefficient, β (1/K)	0.00081

Three distinct five-fin designs are proposed which are categorized based on the branch configurations. Case-1 is an all-straight-fin design but the fins are not uniformly arranged around the circumference of the tube. In case-2 three fins are singly branched at the end. Five variations of this design are studied by simulating different angular arrangements of fins on the tube and the branch angles, thereby achieving an optimized design yielding minimum melting time. Based on this optimized angular orientation of fins and branches, a double branched or leaf-vein patterned design is discussed in Case-3. The schematics of these cases mentioning the important geometric variables are shown in **Figure3.2**.

Geometric details of all the studied cases are shown in **Table 3.2**. Where dimension of all the lengths of fins and branched lengths are shown for all the respective cases. Angles between the main fins and branched are also mention in the table. All the angels are represented by different symbols. Similarly, all inner and outer dimensions for outer shell and inner heat transfer fluid tube is shown clearly in respective table. Thickness of shell and tube also represented in that table. It is pertinent to mention here that for all the studied cases the PCM volume remains fixed in the system; the additional fins and branches are adjusted by reducing/adjusting the thicknesses/lengths of the fins. Case-1 is an all-straight-fin design. In Case-2, three lower fins are single branched at the end. Case-3 comprises of lower three fins as double branched or leaf-vein patterned. Where geometry of all these design of optimum cases are represented in given figure along with detailed dimensions of fins along with their angles are represented in **Figure 3.2**.

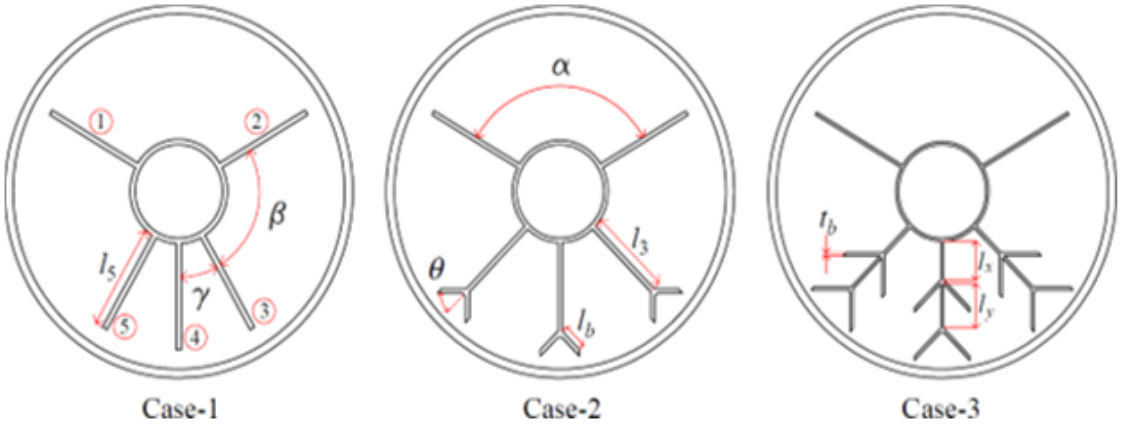

FIGURE 3.2: Schematics of the Three Proposed Five-Fin Designs Named as Case-1, Case-2 and Case-3

Table 3.2: Important Geometrical Dimensions of the Proposed Designs

Case	$\mathbf{t_t}$=$\mathbf{t_f}$=$\mathbf{t_b}$ **(mm)**	$\mathbf{l_1}$=$\mathbf{l_2}$ **(mm)**	$\mathbf{l_3}$=$\mathbf{l_4}$=$\mathbf{l_5}$ **(mm)**	$\mathbf{l_x}$=$\mathbf{l_y}$ **(mm)**	$\mathbf{l_b}$ **(mm)**	α	β	γ	θ
Case-1	1.8	36	36	–	–	120°	90°	30°	–
Case-2	1.5	36	30	–	9	120°	75°	45°	45°
Case-3	1	36	30	15	13.5	120°	75°	45°	45°

3.2 Mathematical Formulation

The flow of the PCM throughout charging and discharging is considered to be unsteady, laminar, incompressible and two-dimensional with negligible viscous dissipation. Thermophysical properties of the PCM and HTF are supposed to be constant over the entire temperature range of operation and Boussinesq approximation is assumed for the density variation of the liquid PCM. It allowed the density to be treated as mean constant density in the governing equations.

Furthermore, volume change during solid-liquid phase change, heat loss at external shell wall and radiative heat transfer are also neglected. The mathematical model for such a problem consists of continuity, momentum and energy equalities uttered as [86].

$$\frac{\partial \rho}{\partial_t} + \frac{\partial u_i}{\partial x_i} = 0 \tag{3.1}$$

$$\frac{\partial \rho u_i}{\partial_t} + \frac{\partial \rho u_i u_i}{\partial x_i} = -\frac{\partial \rho}{\partial x_i} = u\frac{\partial^2 u_i}{\partial x_j^2} + \rho g_i + S_i \tag{3.2}$$

$$\frac{\partial \rho h}{\partial_t} + \frac{\partial \rho u_i h}{\partial x_i} = \frac{\partial}{\partial x_i}(k\frac{\partial T}{\partial x_i}) \tag{3.3}$$

here ρ denotes density of PCM, ρ pressure, gi is representing gravitational acceleration, ui representing fluid velocity, u is representing dynamic viscosity, thermal conductivity is represented by k and h is the sensible enthalpy defined as:

$$h = h_{ref} + \int_{T_{ref}}^{T} C_p dT \tag{3.4}$$

Where reference enthalpy is represented by h_{ref} at the reference temperature T_{ref} defined in the current study as 303 K and Cp is the specific heat. The enthalpy H is then defined as;

$$H = h + \Delta H \tag{3.5}$$

Where ΔH is the latent heat content that varies among zero (for solid) and Lf (for liquid). Natural convection was induced in PCM due to density variation caused by temperature difference and gravity. Therefore, variation in density was attained by using Boussinesq model which treated density as function of temperature and was also applicable where natural convection effects were present. In Boussinesq model variation in density were presented as ρ=ρ_l/((β(T-T_l)+1)), where (β) was thermal expansion coefficient, ρ_l denotes PCM liquidus density and (T-T_l) accounts for temperature difference between liquidus temperature of PCM and tube

temperature. Moreover, k in equation denotes the thermal conductivity, T represents the temperature and h shows enthalpy. Enthalpy of PCM was calculated in three stages with respect to phase of the PCM, (i) when PCM was in sold state below the liquidus temperature (ii) when PCM was neither completely solid nor liquid (iii) when PCM was completely liquid. Variations of enthalpy during above three stages can be mathematically represented.

$$h = \begin{cases} \dfrac{\Delta H}{L_f} = 0, & if\ T < T_S \\ \dfrac{\Delta H}{L_f} = 0, & if\ T > T_l \\ \dfrac{\Delta H}{L_f} = \dfrac{T - T_s}{T_l - T_s}, & if\ T_s < T < T_l \end{cases} \tag{3.6}$$

In the momentum equation, eq (3.2), Si is the Darcy's law damping term added as a source term due to phase change effect on convection. It is defined as

$$S_l = \frac{C(1-\xi)^2}{\xi^2 + \varepsilon}\mu_i \tag{3.7}$$

The coefficient C is a mushy zone constant which generally ranges between 10^4 - 10^7. For the current study its value is 10^5 [57]. The velocity damping in mushy zone is controlled by mushy zone constant C which generally varied between 10^4 to 10^7. The larger values of C induce higher velocity damping which can cause large fluctuations while calculating the solution. In this study, the suitable value of C=10^5 is attained through comparison of experimental and numerical results. A small number ε =0.001 is added in the denominator to ξ^2 in order to avoid the source term to become infinite at ξ=0.

3.3 Numerical Modeling and Grid Convergence

The mathematical model equations governing the melting of the PCM are numerically solved in combination with the initial and boundary conditions for the 2D

planar geometries of different LHTES unit designs using commercial CFD package ANSYS Fluent 19.0. The solver is based on the enthalpy-porosity technique and the finite volume methods as described by Patankar [58]. The geometry is created using Design Modeler sketching tool of the Fluent. Convective terms of the momentum and energy equations are discretized using third order MUSCL scheme whereas diffusion terms are handled using second order central difference schemes. Central differencing can produce non-physical wiggles and unbounded solutions, that leads to reduce accuracy. Third order MUSCL scheme mixtures central differencing and exposed schemes and runs better three-dimensional accurateness and lessens mathematical diffusion. This helps to keep the result stable for a comparatively greater interval step. The PRESTO is applied for the correction of pressure equation, that's suggested method for manipulative natural convection flows [22]. The SIMPLE scheme is employed for pressure-velocity coupling. The under-relaxation factors are chosen as 0.3, 0.2, 0.7, 1, and 0.9 for the pressure, velocity, momentum, energy, and liquid fraction, respectively. Chronological discretization is done by means of second order implicit system thats entirely suitable. The merging standard is set as 10^6 for both the flow and energy equations.

3.4 Numerical Methods

3.4.1 SIMPLE (Semi-Implicit Method for Pressure Linked Equation)

In SIMPLE procedure, relationship between pressure and velocity corrections are used to solve for mass conservation in order to get pressure field. The Simple procedure an iterative aspect process to calculate the pressure field and velocity field. The difficulties related through non linearity for the equation of momentum and link amongst transport equation undertaken through implementing the iterative aspect solution approach.The SIMPLE scheme is employed for pressure -velocity coupling for solving governing equations.

3.4.2 Enthalpy-Porosity Technique

The Enthalpy-porosity method delicacies the meshy (partially solidified region) as a porous medium. The porosity in each cell is set equal to the liquid fraction in that cell. In completely solidified region, the porosity is equal to zero, which covers the velocities in these regions. The main benefit of this method is that it permits a fixed-grid solution of the coupled momentum and energy equations to be assumed deprived of resorting to variable alterations.

3.4.3 Third-Order MUSCL Scheme

Third-order MUSCL scheme is derived from the original MUSCL (Monotone Upstream-Centered Scheme for Conservation Laws) by adding a blending function into second order upwind scheme and central differencing scheme. Central differencing scheme can produce non-physical wiggles and unbounded solutions, which can therefore lead to stability problems and compared to the second order upwind scheme.

3.4.4 PISO (Pressure Implicit with Splitting of Operator)

The PISO process is non iterative aspect transient process that's depends on time-based accurateness attained through discretization exercise. It is transient procedure having all time dependent relations taken in the equation of momentum and continuity. That outcomes the further contribution to corrective equations of pressure and momentum in the transient formula. The field of pressure and velocity got at the final step of PISO process with the minor time step are used and these steps are precise enough to continue for next time step.

3.5 Initial and Boundary Conditions

At time t = 0, temperature of the PCM is initialized as 303 K. The HTF flows through the tube at constant temperature of 358 K, therefore, the inner wall is

assumed to be isothermal at the same temperature, i.e., 358 K. At the external surface of the tube coupled boundary condition is applied which links the temperature difference of the external surface of Heat Transfer Fluid duct with that of the Phase Change Material. Considering the conductivity of the outer shell which assists in the melting of the PCM as well, a thermal combined boundary situation is also applied at inner surface of the shell which is the interface between the Phase Change Material and shell. To avoid heat loss from the system, the external surface of the shell is insulated, therefore, adiabatic wall boundary condition is applied. The initial and boundary conditions are schematically shown in **Figure: 3.3**.

3.6 Grid Convergence

A grid convergence study is done to select a suitable grid and time-step resolution for the present numerical analysis. We selected one of the proposed design geometry to perform this analysis and suitable grid and time step applied to all other proposed designs. Three different grid sizes with 10000, 20000 and 40000 computational cells are used and named as coarse, medium and fine, respectively.

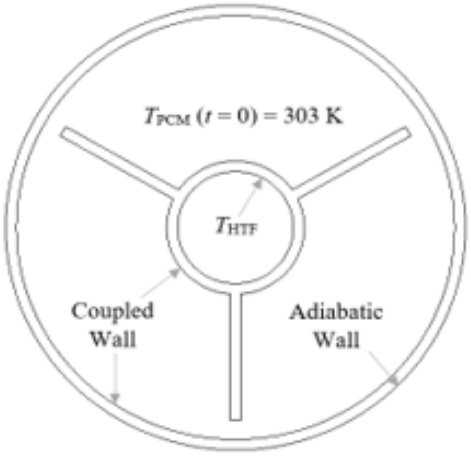

FIGURE 3.3: Schematic Representation of the Applied Primary and Boundary Conditions

The temporal variation of the average temperature and melting fraction of the PCM is plotted for the three grid resolutions as shown in **Figure: 3.4**. The

trends of both the parameters show little or no variations with the grid refinement, therefore, medium size is selected for the subsequent studies. The outcome of interval-step size on the results is also inspected by equating the results against different time-step resolutions. It is observed that the simulations become unbalanced for interval-step size greater than 250 ms, therefore, 100 ms is selected for all the simulations to follow.

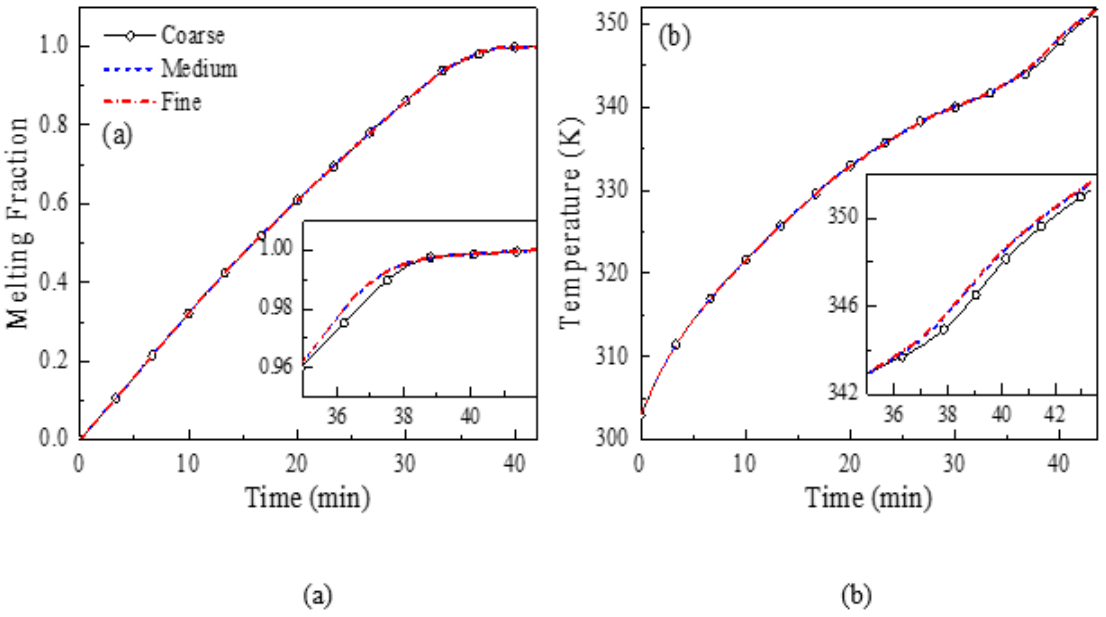

FIGURE 3.4: Grid Convergence Study Showing the Time History of (A) Average Temperature and (B) Melting Fraction for Three Grid Resolutions for the Case-3 Design

3.7 Numerical Model Validation

Before proceeding to the detailed numerical studies, the present numerical model and solution technique is first validated by comparing the simulation results with the experimental data. An experimental test bench is setup for this purpose.

3.8 Experimental Setup

The investigational setup contains a horizontally configured concentric shell and

tube type LHTES system as shown in **Figure: 3.5**. It comprises of a LHTES unit, hot water storing chamber, warm water rotation pump, electronic temperature controller, flow meter, data acquisition and display system and by hand operated valves. Phase Change Material used is selected Stearic acid while water is the HTF. Three fins are uniformly arranged in Y-configuration around the HTF tube to enhance the heat transfer between HTF and PCM. Hot water is maintained at a constant temperature by using 3 heating system of 1500 W each and a temperature regulator. A 372 W pump circulates the warm liquid by the circuit at a flowrate of 0.441 kg/s. A total of six thermocouples are installed at two different cross-sections to quantity the temperature of PCM in latent heat storage unit. These thermocouples are inserted 25 mm radially into the shell and are installed in among the fins as shown in **Figure: 3.6**. Two further thermo couple junction; one each at inlet and outlet of the latent heat storage unit; are used to measure the temperature drop across the unit.

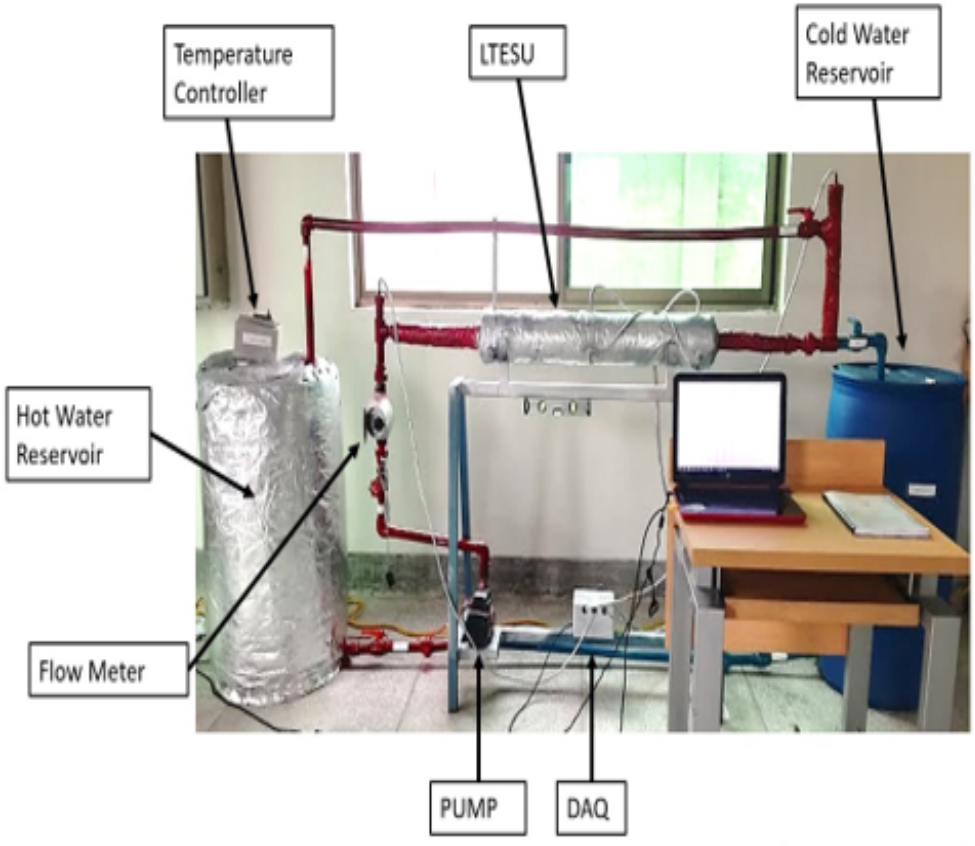

FIGURE 3.5: Experimental Setup of the Latent Heat Thermal Energy Storage (LHTES) System

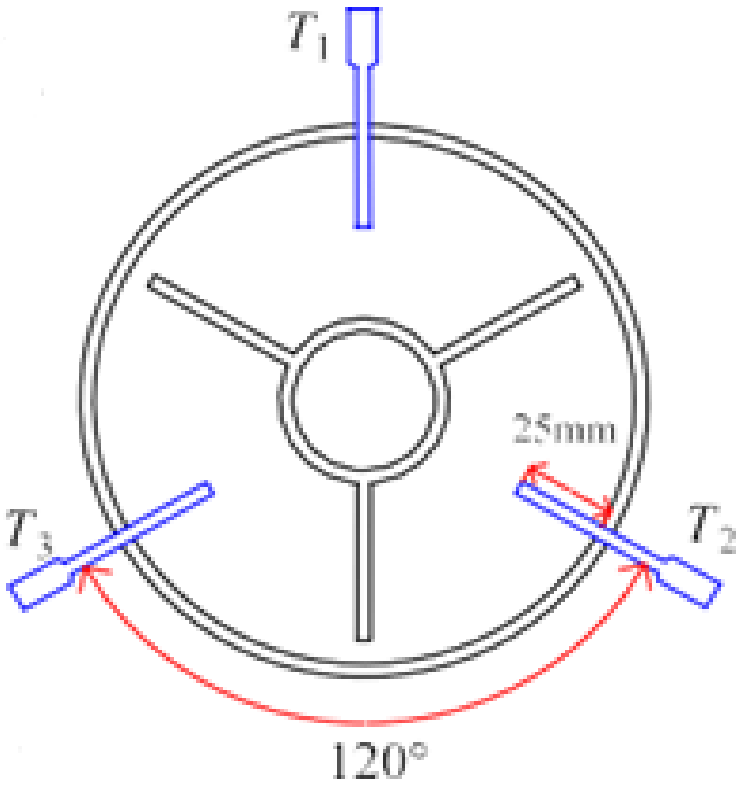

FIGURE 3.6: Schematic Representation of the Thermocouples Installed at One of the Cross-Sections of the Latent Heat Storage Unit

3.9 Comparison of the Numerical and Experimental Results

The numerical study of PCM melting in the latent heat storage unit is performed for a 2D planar geometry assuming the temperature changes in the third dimension as negligible. In order to justify this assumption, the temperatures of HTF at the inlet and outlet of the LHTES unit are measured experimentally. It is observed that the HTF temperature stays approximately constant at 358 K at both ends of the unit during the melting operation as shown in **Figure: 3.7**. The maximum temperature change is observed during the initial times where it is as high as 4 K. However, the average temperature difference is 0.5 K for the whole cycle which is negligible and therefore justifies our 2D assumption for the numerical analysis. The numerical results are measured at the same locations as experiments by defining probes at the points where thermostats are installed.

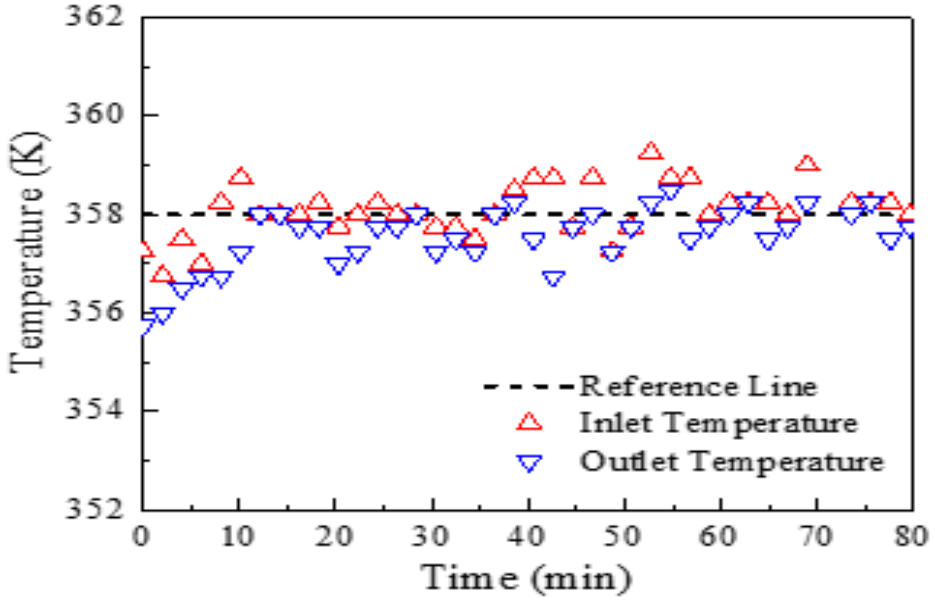

FIGURE 3.7: Heat Transfer Fluid Temperatures at the Inlet and Outlet of LHTES Unit

The temporal variation of the average temperature of PCM and the melting fraction is plotted for both the simulations and the current experimental studies as represented in **Figure: 3.8**. The mathematical outcomes show an outstanding arrangement with the experiments, thereby, validating our numerical model and solution strategy.

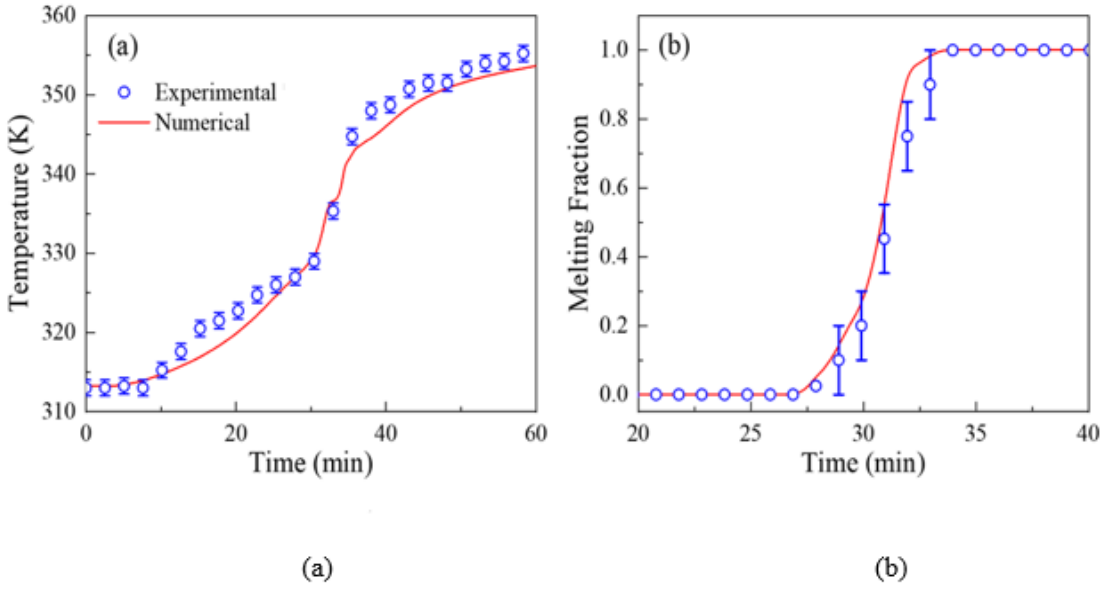

FIGURE 3.8: Evaluation of the Experimental and Mathematical Results for the Temporal Difference of (A) Average Temperature and (B) Melting Fraction for the Y-Oriented Triple-Fin Design

The current numerical solution strategy is further validated by setting up and simulating several test cases identical to those available in the literature. Al-Abidi et al. performed both the experimental and numerical studies for the melting [20] and solidification [21] of RT82 used as Phase change material in a horizontally configured triplex tube heat exchanger with internal and external fins. **Figure: 3.9** shows the comparison of our numerical results with the investigational and mathematical results of Al-Abidi for the temporal distinction of PCM average temperature for charging and discharging processes. An excellent agreement is observed among the current numerical outcomes and the numerical outcomes of Al-Abidi verifying our numerical approach. The present numerical results also compare well with the experimental results validating and verifying our mathematical model and numerical discretization techniques.

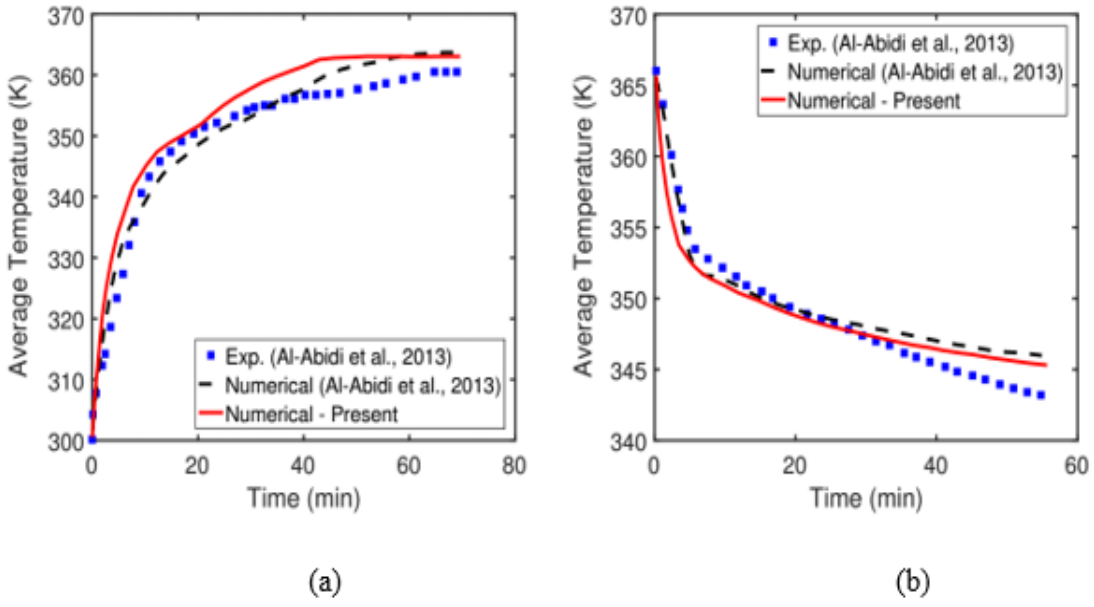

FIGURE 3.9: Comparison of the Present Numerical Results with the Experimental and Numerical Results of Al-Abidi Et Al. [20],[21] for the time Variation of Average Temperatures During (A) Melting and (B) Solidification of the PCM in a Triplex Tube Heat Exchanger

Chapter 4

Results and Discussion

Simulation cases are setup for the base case and the three proposed fin designs; geometric features, initial and boundary conditions are specified as discussed in previous sections. Simulation studies are performed for several design conditions and the outcomes are analyzed for the temperature transmission and melting enhancement. Different performance enhancement indicators are discussed and the best design is identified. The energy storage capacity and energy storage rates for different designs are discussed. Furthermore, the effects of the thermophysical properties of the fins and shell materials on the melting enhancement are also discussed. The effect of HTF temperature on the melting is presented using non-dimensional Stefan, Nusselt and Rayleigh numbers.

4.1 Contour Plots of Melting Fraction, Temperature and Velocity

Contour plots of melting fraction for the base case and the three new designs at different times through the melting procedure are shown in **Figure: 4.1a**. Rows correspond to different designs whereas the columns represent different time levels during the melting. As the HTF flows through the tube, it conducts heat to the PCM through the walls of the tube and the fins, thereby, melting the PCM;

conduction being the dominant heat transfer phenomena. The melted PCM starts rising upwards due to buoyancy effects creating convective currents. These convective currents speedup the melting process by agitating the PCM. The base case analysis reveals that the single fin extending vertically downward is not enough to melt the whole body of PCM in the lower half portion of the LHTES unit. This is because the convective currents; which now govern the heat transfer; sweep upwards alongside the lower vertical fin without disturbing the major portion of PCM in the lower half portion. To cope with this situation, Case-1 design is proposed with three fins replacing the single fin in the lower half section. The included angle of the fins is 30°. A clear melting enhancement can be observed from the contour plots of melting fraction. It takes now 61.7 minutes to completely melts the PCM as compared to 80 minutes for the base case: 1.3 times faster melting. An avenue for the further improvement can be seen looking at the melting behavior: vary the fins included angle and branch the fins; Case-2 is the output.

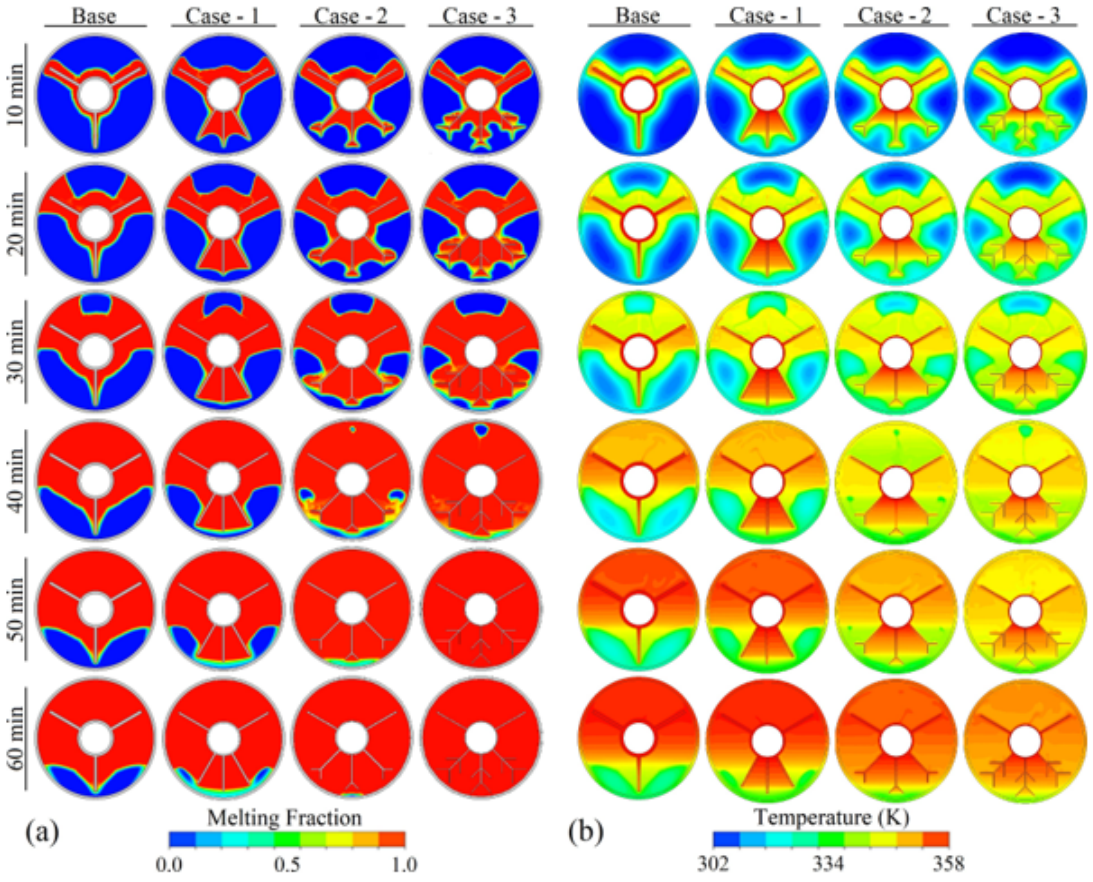

FIGURE 4.1: Contours Plots of Melting Fraction for the Base Case and the New Proposed Designs at Different Times During the Melting Process

A parametric study is performed by varying the fins included angle 'γ' and the branch included angle 'Δ' to obtain an optimum value. It is observed that 45° is the optimum value at which maximum enhancement is achieved. For the Case-2 the PCM completely melts in 51.7 minutes: 1.55 times faster melting as compared to base case. However, it can be seen that there are still some pockets of solid PCM between the upper fins and the lower fins which can be handled using a double-branched or leaf-vein patterned design for the three lower fins. Case-3 is based on that fin-design yielding effective melting of these solid pockets as shown in the 4^{th} row of **Figure: 4.1**. The whole PCM melts in 43.3 minutes which is 1.85 times faster as compared to the base case. To analyze the temperature distribution in the LHTES unit, temperature contours are plotted for all the cases at the same time instances as for the melting fraction as shown in **Figure: 4.1(b)**. These contours reflect the low temperature regions where the PCM remains solid and guide for a fin design to achieve better heat transfer and melting enhancement. The temperature contours of the base case clearly show the low temperature regions in the lower half portion of the unit. As we improve the design by increasing the number of fins in the lower half portion and subsequently branching them, the temperature distribution also improves and for the double branched or leaf-vein patterned design an almost uniform temperature distribution is achieved through out the cross-section of the unit.

To further explore the temperature variation and melting process, line plots of average temperature and melting fraction are plotted over the melting time span for all the four cases as shown in **Figure: 4.2**. Both the parameters show a change in the slope between 30 – 40-minute interval. This is attributed to the fact that till 35 minutes all the PCM in the upper potion gets melted due to the dominating convection effects.

After that the remaining PCM settling down in the bottom section of the unit slowly melts due to the conduction heat transfer. This is reflected by the decreased slope of the melting fraction curve after 35 minutes. As the PCM melting slows down, more heat contributes towards temperature rise as shown by sudden jump in the temperature curves as shown in **Figure: 4.2 (b)**.

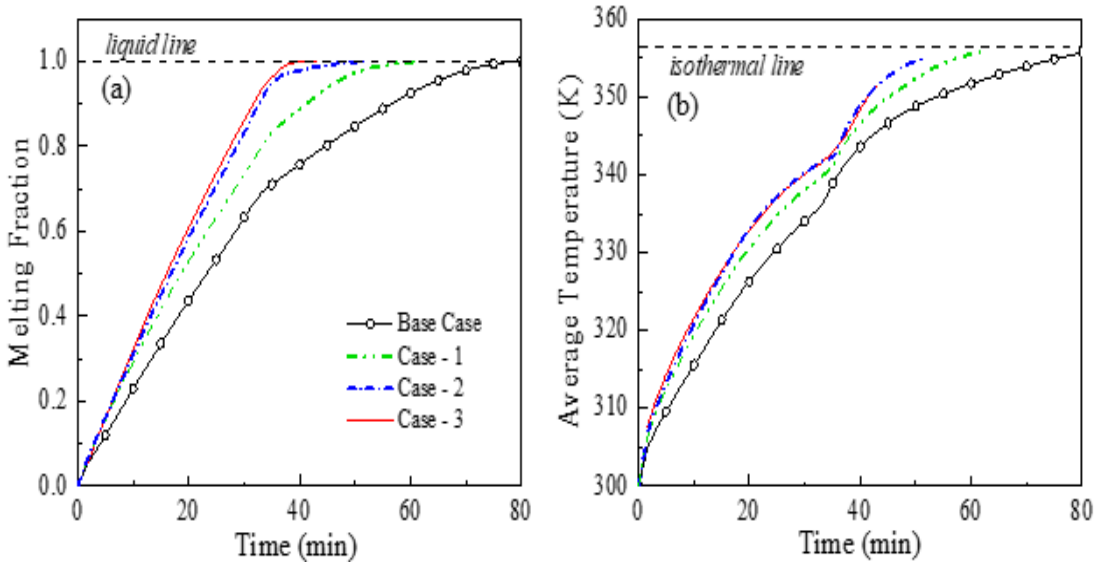

FIGURE 4.2: Line Plots of (A) Average Temperature and (B) Melting Fraction for the Base Case and the New Proposed Designs Plotted Over the Time Span of the Melting Process

To further reinforce the visualization of melting process, the contour plots of velocity are shown in **Figure: 4.2**. The contour lines of velocity clearly show the propagating melting front of the PCM.

During the initial stages of melting these contour lines envelope the melted PCM around the HTF tube and fins. As the PCM continues to melt and starts rising upwards due to buoyancy, the velocity contours lines also develop around the melted PCM body. The maximum velocities appear in the melted PCM between the two upper fins.

For the Y- oriented triple-fin base case and the Case-1, velocities sweep alongside the lower fins and are concentrated in the upper portion later on whereas for Case-2 and Case-3 velocities are more distributed in the whole domain due to branched fin heat transfer and melting enhancement.

4.2 Melting Enhancement Indicators

Two indicators are defined to quantitatively analyze the heat transfer and melting enhancement of the proposed fin designs for the melting of PCM. These are percentage melting enhancement 'η' and the percentage time saving 'τ'. Percentage

melting enhancement is defined as:

$$\eta = \frac{\phi_i(t) - \phi_0(t)}{1.0} \times 100 \tag{4.1}$$

Where $\phi_i(t)$ is the melting fraction of the proposed fin design case at time t and $\phi_0(t)$is the melting fraction of the base case at the same time t. **Figure: 4.5(a)** shows the plot of η against time for the three proposed designs. For all three designs *tau* increases, achieves a maximum value and then decreases. Case-1 and Case-2 achieve maximum enhancement at 40 minutes whereas Case-3 achieves the same at 30 minutes. This is due to the fact that Case-3 cause faster melting and reports enhancement quicker. On the base of these two parameters case-3 is optimum design for the present study.

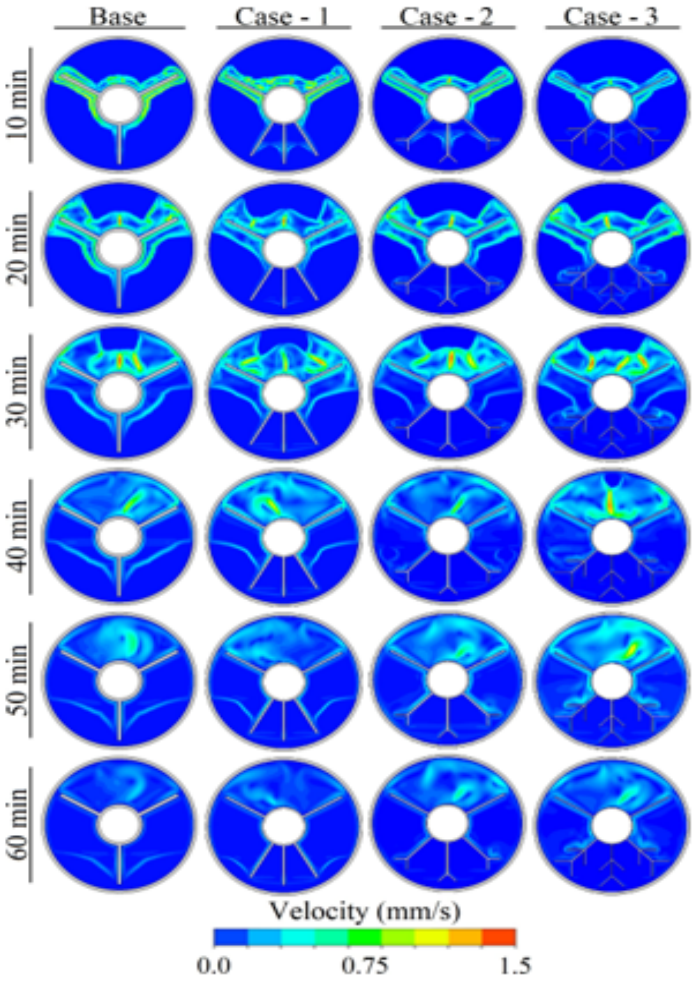

FIGURE 4.3: Contour Plots of Velocity for the Base Case and the New Proposed Designs at Different Times During the Melting Process

Percentage time saving τ expresses the percentage of time saved comparative to the base case because of the faster melting. It is defined as;

$$\tau = \frac{t_{m,0} - t_{m,i}}{t_{m,0}} \times 100 \tag{4.2}$$

Where $t_{m,0}$ and $t_{m,i}$ represents the time required for the total melting of Phase change material for base case and new designed case, respectively. **Figure: 4.4(b)** shows the bar chart representing the percentage time savage for the different cases. Case-3 design quickly melts the PCM saving 45.9% time compared to the base case.

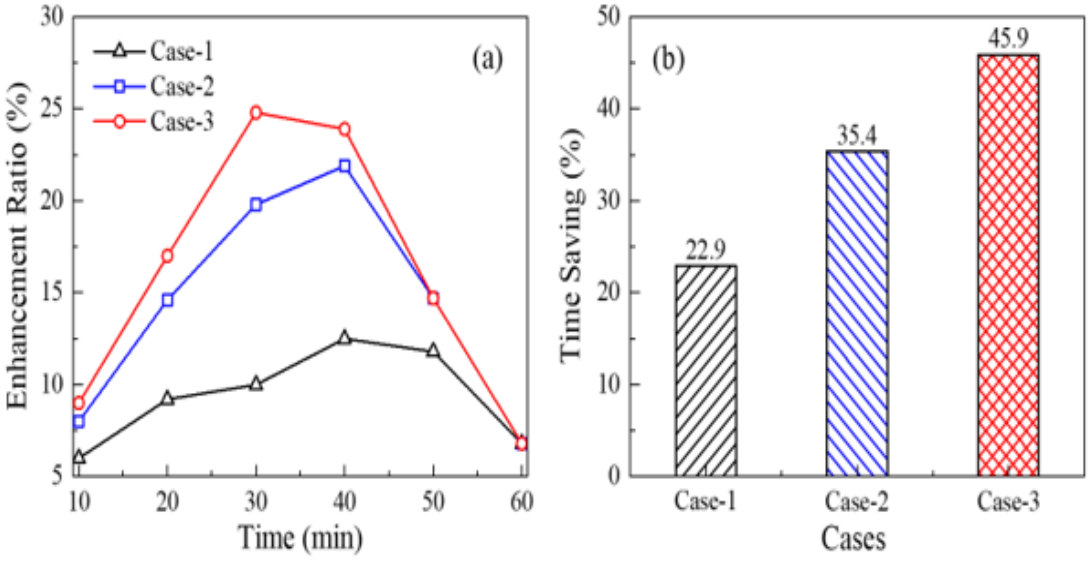

FIGURE 4.4: (A) Percentage Melting Enhancement and (B) Percentage Time Saving Achieved Using Three New Proposed Designs

4.3 Total Energy Storage and the Storage Rate for Melting

Total energy stored by the PCM in a particular time span is a direct measure of the design effectiveness. **Figure: 4.5(a)** shows the energy stored by different designs at three instances of time. It is observed that for all the times presented, Case-3 stores maximum energy followed by Case-2, Case-1 and the base case. At complete melting of the respective cases, Case-3 stores maximum energy of 3600

kJ which is the maximum storage capacity of the LHTES unit. Case-1, on the other hand, stores only 3000 kJ energy when completely melted. **Figure: 4.5 (b)** shows the energy storage rates for all the cases. Initially, the energy storage rate of all the new designs are higher as compared to the base case. This is because these designs have more surface area for heat transfer due to a greater number of fins. Afterwards, there is a continuously decreasing trend of the energy storage rate for all the case. This is due to the fact that there is more temperature gradient at start, which decreases as the PCM melts therefore decreasing transfer of heat between the heated surfaces and the PCM. Several depressions are also observed in the energy storage rate curves which are attributed to the complex interactions of the flow eddies and convective currents with the heated surfaces and the PCM body.

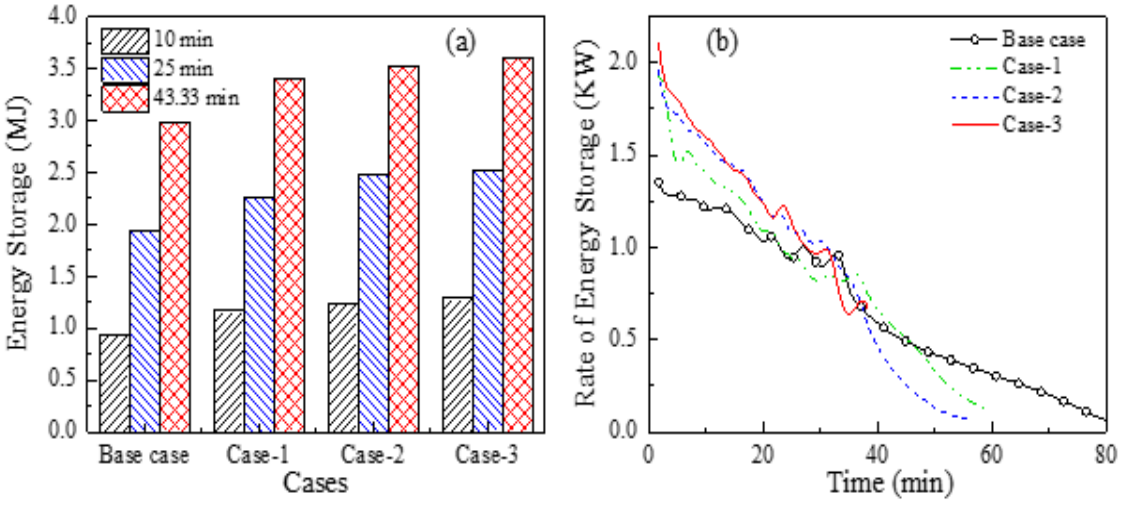

FIGURE 4.5: (A) Total Energy Stored and (B) the Rate of Energy Storage for All the Studied Cases

4.4 Effect of the Fin and Shell Material on Melting of PCM

Three test cases are simulated by using copper, aluminum and steel as fin materials for the Case-3 to analyze the effects of thermophysical properties of fins on the melting behavior. The properties of the three selected materials are shown in

Table 4.4. Results show that copper is the best option as fin material giving faster melting as compared to the other two choices as shown in **Figure: 4.6 (a)**. The reason being the better thermal diffusivity and thermal effusivity of the Copper as compared to the other two materials tested, i.e., it betters conducts heat and quickly transmits it to the surroundings, respectively.

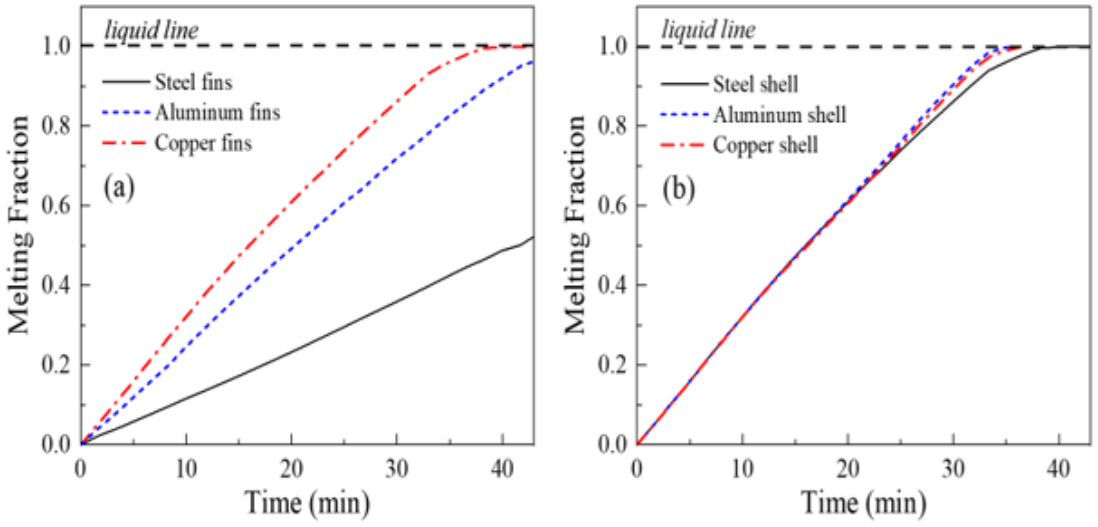

FIGURE 4.6: Melting Fraction of PCM Plotted Against Time for the Case-3 Design Using Different (A) Fin and (B) Shell Materials

Deng et al. [88] discussed the effects of shell conduction on the melting enhancement of the PCM in comparison with the isolated shell and reported that the shell conductance sufficiently enhance the melting of PCM. It supports the idea that a highly conducting shell will also accelerate the melting process. Therefore, the effects of the thermophysical properties of shell are studied using copper, aluminium and steel as the shell materials for the Case-3 design.

The comparative results of the liquid fraction of shell materials are shown in **Figure: 4.7(b)**. During the initial 20 minutes where 60% of the PCM gets melted, there is no effect of the shell material on the melting trend. Afterwards, the unit with copper and aluminium shells continue melting on faster pace whereas the unit with steel shell slows down. This is because when PCM melts, it rises upwards due to buoyancy and the convective currents causes the liquifying whole PCM in the top portion of given unit. The melted PCM is now in contact with the shell and transfers heat to the shell.

TABLE 4.1: Thermophysical Properties of Fin and Shell Materials

Properties	**Steel**	**Aluminium**	**Copper**
Thermal Conductivity (W/m.K)	16.27	202.4	387.6
Specific heat (J/kgK)	8030	2179	8798
Specific heat (J/kgK)	502.5	871	381
Thermal diffusivity (mm^2/s)	4.03	106.6	115.6
Thermal effusivity ($W/cm^2Ks^{-0.5}$)	0.81	1.96	3.61

The heat is now conducted through the shell towards the lower section of shell which is at lower temperature and contains solid body of PCM which now starts melting. A shell with high thermal diffusivity will quickly conduct heat to the lower portion of the shell as in the case of aluminium and copper. It takes 37 minutes to melt the whole PCM with copper and aluminium shells whereas 43 minutes with steel shell, i.e., 53.75% time savage or 2.16 times faster melting/charging as compared to the base case.

4.5 HTF Temperature Effects on Melting of PCM

The HTF temperature directly effects the melting time of phase change material in the latent heat storage unit. An increase in temperature of the HTF increases the temperature difference between the heated tube and the PCM thereby enhancing

the melting rate. Stefan number (Ste) is the relevant non-dimensional number defined as;

$$Ste = \frac{Cp_l(T - T_l)}{L_f} \tag{4.3}$$

Where T is the temperature of the HTF which is implemented in the numerical solution as an isothermal boundary condition of the inner surface of the tube and is varied between 340 K – 368 K with an interval of 4 K. The corresponding Stefan number varies in the range 0.0514 – 0.289. The remaining terms in Eq. (10) have their usual meaning as given in **Table: 4.1**.

Figure: 4.7 (a) shows the plot of melting time for various Stefan numbers for the Case-3 design using Steel and Copper as the tube materials. The melting time decrease as we increase the Stefan number. This decreasing trend is exponential in the Stefan number range of $0.05 < \text{Ste} < 0.2$ which slows down and becomes linear afterwards. This is because the melted PCM forms an envelope around the heated surfaces therefore reducing the conduction heat transfer. However, the efficient double branched design continues to transfer heat and promotes melting by generating convective currents when conduction slows down due to thick molten boundary layer of PCM. This is shown in **Figure: 4.7 (b)** where average Nusselt number $\overline{Nu}$ is plotted against the Rayleigh number Ra for two different tube materials. $\overline{Nu}$ is the proportion of the convection to the conduction heat transfer and is calculated as;

$$\overline{Nu} = \frac{\dot{Q}}{\pi k_{PCM}(T - T_{PCM_i})} \tag{4.4}$$

Where $\dot{Q}$ representing average energy rate stored by the phase change material and considered as the overall energy stored divided by the whole melting rate. $T_{PCM,i}$ represents the initial temperature of the PCM. Rayleigh number is the proportion of buoyancy to viscous forces and is calculated as:

$$Ra = \frac{g\kappa(T - T_l)D_t^3}{\nu_l \sigma_{th,l}} \tag{4.5}$$

Where κ is the thermal expansion coefficient, and ν_l and

$\sigma_{th,l}$ represents the kinematic viscosity and the thermal diffusivity of the liquid PCM, respectively. An increase in the temperature of HTF increases Ra thereby increasing the buoyancy forces which creates convective current which in turn causes an increase in the $\overline{Nu}$ as shown in **Figure: 4.7 (b)**.

A change in tM as a function of Ste, and variation in Nu as a function of Ra can be estimated using the correlations presented in Equation 13 and 14. The estimations offered by these correlations are plotted as dashed lines alongside the numerical results in figure.

$$t_M = a(St)^{-0.55} \tag{4.6}$$

$$\overline{Nu} = 11.75In(Ra) - b \tag{4.7}$$

The values of curve fitting constants a and b in Equation (15) are a = 28.4, b = 147.88 for steel, and a = 25.4, b = 152.03 for copper. These correlations match well with the reference data for both tube materials as evident from Figure: 4.9.

4.6 Contour Plots of Melting Fraction and Temperature for Solidification

Contour plots of melting fraction for all the cases at different time instances during the solidification process are represented in **Figure: 4.8**. As the charging process completes, constant temperature 300 K is now given to the HTF tube that is lesser than the melting temperature of the PCM. The HTF tube and the fins and branches are now cooler than the PCM. Therefore, the heat is conducted from the PCM to the HTF. The temperature of the HTF starts increasing and that of the PCM starts decreasing. When the temperature of the PCM approaches the solidus temperature, the PCM starts solidifying. This is represented by the blue contours

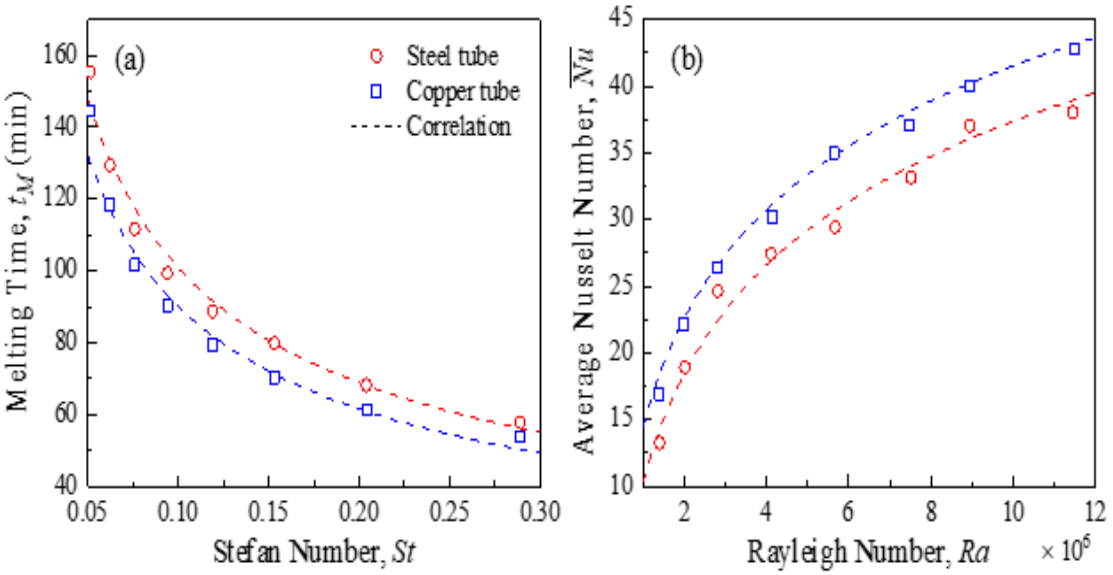

FIGURE 4.7: Effects Of HTF Temperature on the System Performance Using Two Different Tube Materials (A) Complete Melting Time is Plotted Against Various Stefan Numbers, (B) Average Nusselt Number is Plotted Against Rayleigh Number

of liquid fraction as shown in **Figure: 4.8** near the HTF and the fins which subsequently advances as the time progresses. The PCM starts solidifying near the HTF tube and the fins. The base case with the single fin extending vertically downward is not having enough heat transfer surfaces to solidify the whole body of PCM efficiently. In contrast, all the new proposed designs perform better than the base case extracting heat quickly from the liquid PCM and therefore solidifying it. Since the solidification is conduction dominant phenomenon, therefore, the design with more heat transfer surface area is expected to perform better. This is the reason that Case-3 is the most efficient design for solidification process too. It takes 239 minutes for the base case to solidify the whole body of PCM as shown in **Figure: 11(a)**, which represents the line plots of liquid fraction varied over time. Case-1, Case-2 and Case-3 take 236 minutes, 229 minutes and 220 minutes, respectively, to completely solidify the PCM. The reason of the faster solidification for the proposed cases is the more surface area available for the heat transfer.

The contour plots of temperature for the base case and the modified designs are shown in **Figure: 4.9** which also justifies our discussion made on the liquid fraction contours.

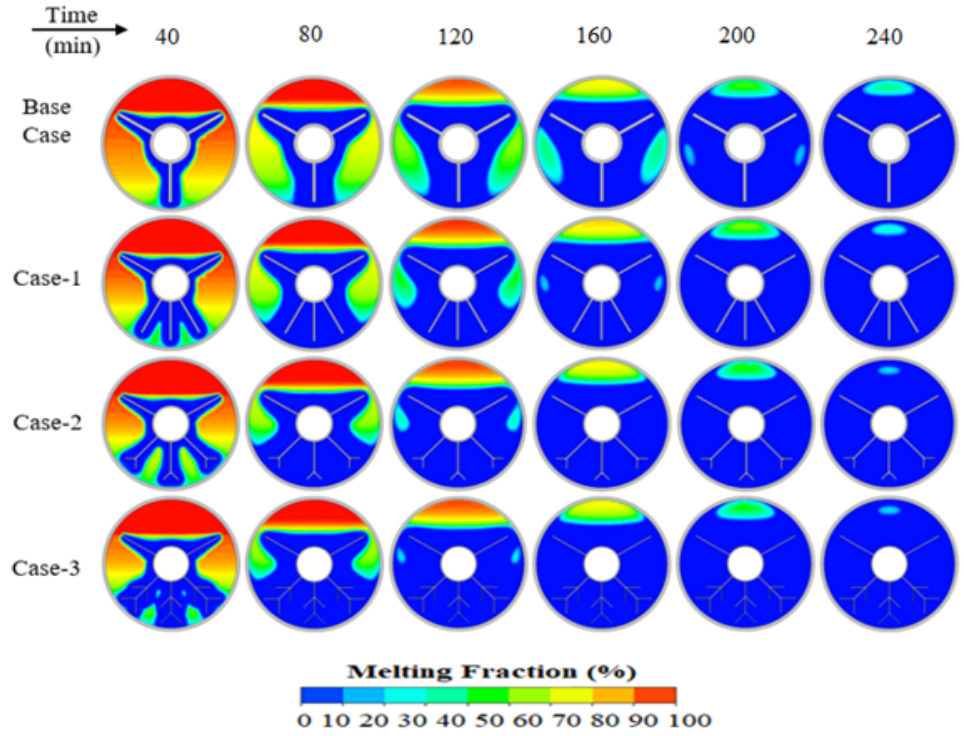

FIGURE 4.8: Contours Plots of Solidification Fraction for the Base Case and the New Proposed Designs

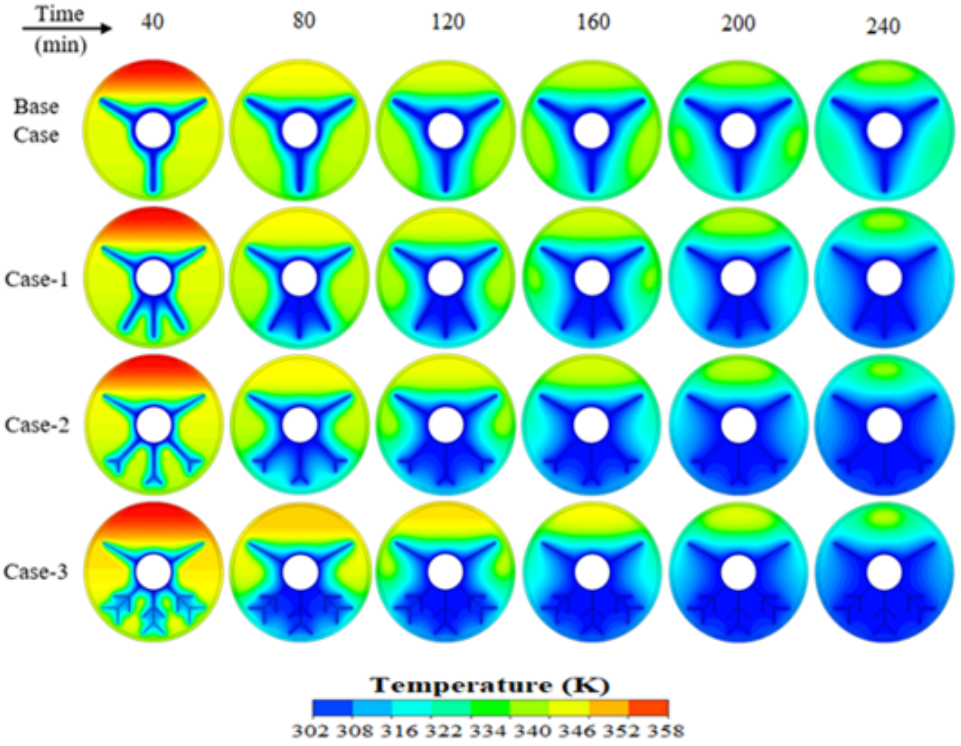

FIGURE 4.9: Contour Plots 0f Temperature for the Base Case and the New Proposed Designs

The temperature contours clearly show low temperatures produced in the PCM near the HTF tube and the fins because the HTF absorbs heat from the PCM. When the temperature reaches the solidus temperature, i.e., 327 K, the PCM starts to solidify. The low temperatures slowly advance in the whole PCM and solidifies it. Case-3 is having more heat transfer surface area and therefore absorb heat more rapidly and uniformly from most of the PCM body through conduction heat transfer. The line plots of the average temperature variation with time for all the cases are shown in **Figure: 4.10 (b)**. Since only mode of heat transfer is the conduction, therefore, the average temperature profiles are almost the same for all the cases. The average temperatures decrease sharply in the beginning because of large temperature gradients initially between the HTF and the liquid PCM direct in contact with the HTF tube. Later on, the average temperature decrease follows a linear trend.

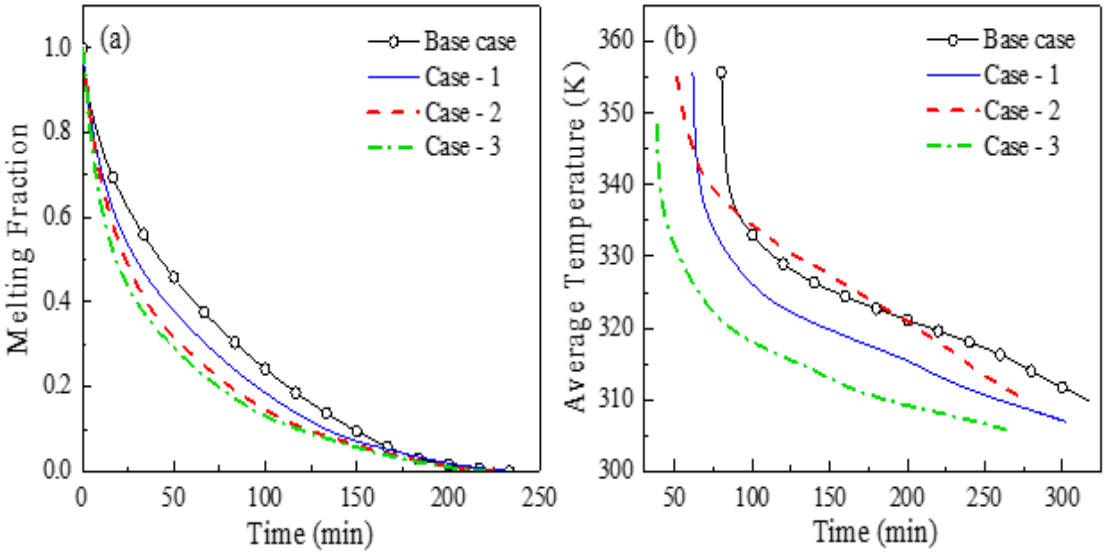

FIGURE 4.10: Plots of (A) Melting Fraction for Solidification and (B) Solidification Temperature for the Base Case and the New Proposed Designs

4.7 Complete Melting-Solidification Cycle

Numerical studies are also performed for the base case and the modified fin designs to examine the complete melting and solidification cycle of the Phase change

materials. Temporal variation of the melting fraction and average temperature are shown in **Figure: 4.11**. Total melting-solidification time for the base case is 318 minutes while for all optimum cases is it is 301 minutes, 280 minutes and 263 minutes, respectively. Case-3 performed best for the reasons discussed earlier.

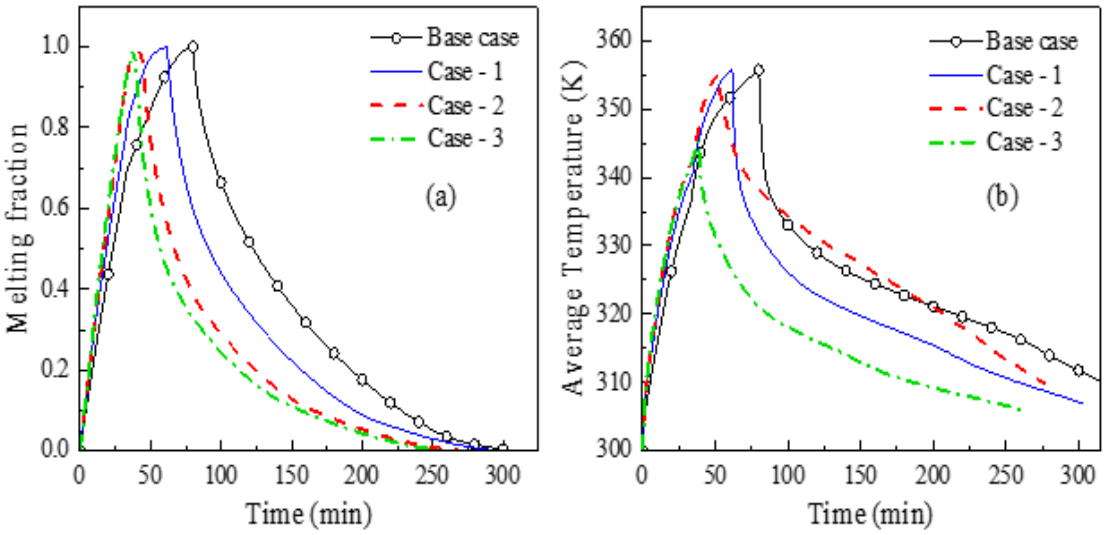

FIGURE 4.11: Plots of (A) Melting Fraction For Total Melting and Solidification and (B) Solidification Temperature for the Base Case and the New Proposed Designs

4.8 Performance Indicators for the Complete Melting-Solidification Cycle

Percentage enhancement 'η' and the percentage time saving 'τ' are used as performance indicators to analyze the performance of the proposed designs against the base case for the complete melting-solidification cycle. **Figure: 4.12 (a)** shows the plot of 'η' against time for the three proposed designs.

For all three designs, percentage enhancement ratio shows two spikes. All the cases achieve their maximum percentage enhancement ratio at 80 minutes whereas Case-3 goes to maximum value of 60% as compare to Case-1 and Case-2 that attain 49% and 35%, respectively, at that time. This is due to the fact that Case-3 cause faster melting and solidification.

Figure: 4.12 (b) shows the bar chart representing the percentage time savage for the proposed new designs against the base case. Case-3 design is the best among the proposed design which quickly completes the melting-solidification cycle saving 17.29% time compared to the base case. Case-1 and Case-2 show percentage time saving values of 5.34% and 11.94%, respectively.

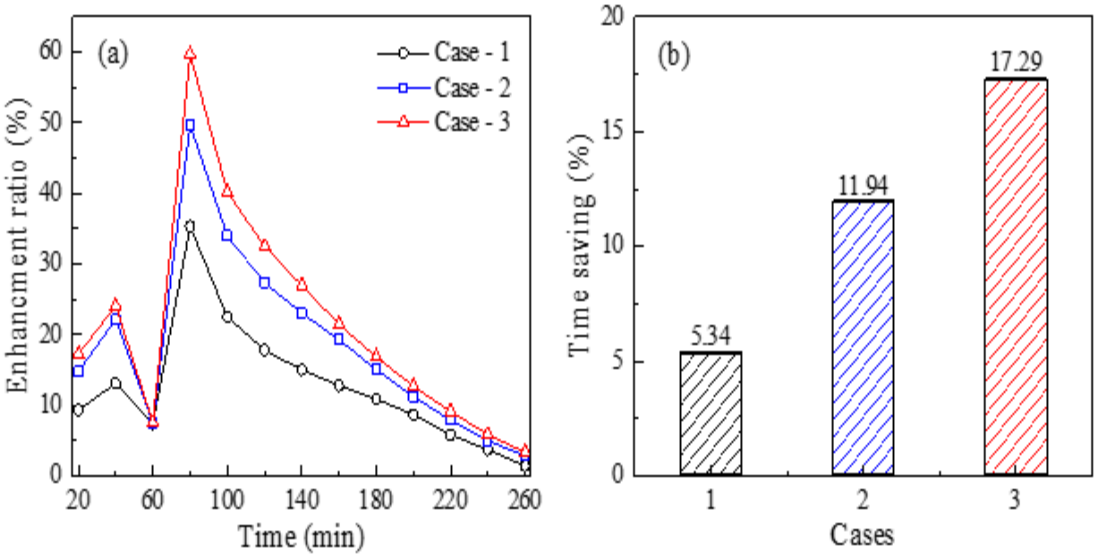

FIGURE 4.12: (a) Total Time Saving for Complete Melting and Solidification (B) Enhancement Ratio for Complete Melting and Solidification

4.9 Effects of Nano-Particles on Melting and Solidification

The study aims to investigate the melting and solidification process of nanoparticle-enhanced phase change material (NEPCM) filled in a LHTES system. In the literature it is discussed that different type of metallic oxide can be mixed with the PCM in different concentrations to enhance the thermal conductivity of the PCM. In the current study aluminum oxide (Al_2O_3) is selected as a Nano-particle. The LHTES unit consists of a shell filled with stearic acid as PCM dispersed with high conductivity nanoparticles (Al_2O_3). Nano-particles are used in concentrations of 1%, 5%, and 10%. The model equations used to find the properties of Nano-particles are discussed below.

4.9.1 Density and Specific Heat

Specific heats and Density of the Nano-particles mixed PCM are calculated equations 4.8 and 4.9 respectively [89]. Where ϕ is fraction of aluminum oxide that are added in base PCM. Where left terms of equation give us the value of specific heat and density by combing the respective density and specific heats of base PCM and nanoparticles.

$$(\rho C_p)_{NEPCM} = (1-\varphi)(\rho C_p)_{PCM} + \varphi(\rho C_p)_{NP} \tag{4.8}$$

$$(\rho)_{NEPCM} = (1-\varphi)\rho_{PCM} + \rho_{NP}\varphi \tag{4.9}$$

4.9.2 Latent heat, thermal conductivity and dynamic viscosity

Latent heat, thermal conductivity and dynamic viscosity of Nano-particles mixed PCM are calculated using equations 4.10, 4.11 and 4.12 respectively. Where latent heat and dynamic viscosity is depending upon the percentage of nanoparticles used while calculation of thermal conductivity involves the function of thermal conductivity of base PCM and thermal conductivity of nanoparticle with the percentage of nanoparticle used.

$$(\rho L)_{NEPCM} = (1-\varphi)\rho L_{PCM} \tag{4.10}$$

$$\kappa_{NEPCM} = \frac{\kappa_{NP} + 2\kappa_{PCM} - 2\varphi(\kappa_{PCM} - \kappa_{NP})}{\kappa_{NP} + 2\kappa_{PCM} + \varphi(\kappa_{PCM} - \kappa_{NP})}\kappa_{PCM} \tag{4.11}$$

$$\mu_{NEPCM} = \frac{\mu_{PCM}}{(1-\varphi)^{2.5}} \tag{4.12}$$

4.10 Effects of Nano-Particles on Melting Fraction and Temperature Profiles

Al2O3 nanoparticles are highly conductive and their addition in the PCM can significantly enhance its thermal conductivity. The increased thermal conductivity in turn increases the conduction heat transfer rates during the entire melting process, resulting in faster melting. Specifically, it plays a dominant role during the initial melting phase. **Figure: 4.12** shows the improvement in melting fraction and temperature (TPCM) as a function of time with the addition of nanoparticles in the PCM for Case-3. Faster melting rates can be observed with higher concentrations of NEPCM owing to its greater thermal conductivity. Moreover, the NEPCM cases are observed to melt faster through- out the melting process. The whole body of the NEPCM melts in 38.3 min, 35 min and 31.7 min for cases with 1%, 5% and 10% concentrations of nanoparticles, respectively, as compared to 43.3 min of Case-3 with pure PCM.

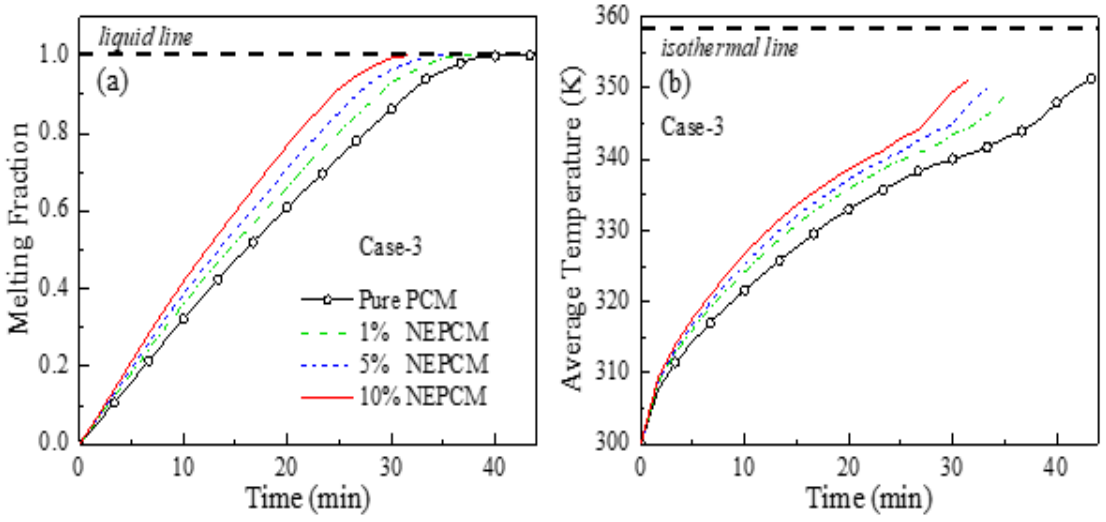

FIGURE 4.13: Comparison of (A) Melting Fraction and (B) Average Temperature Plotted Against Time for Different Concentrations of Nanoparticles Added in the PCM Using the Geometry of Case-3

Furthermore, the average temperature of the NEPCM increases rapidly through increasing in the percentage of nanoparticles, even though, the final average temperature values are not much different as evident from **Figure: 4.15(b)**. This is a consequence of a progressive increase in thermal conductivity with an increase in nanoparticle concentration, thereby enhancing heat transfer; causing a rapid rise in temperature. Moreover, 1% NEPCM is seen to attain the lowest average temperature when completely molten while 10% NEPCM is seen to attain the maximum. This is because specific heat of the NEPCM decreases as the concentration of nanoparticles is increased. Therefore, for the same amount of energy, the average temperature of 10% NEPCM rises more as compared to the case with 1% NEPCM.

Table 4.2: Properties of Nano-PCM

Concentration	**Density (Kg/m3)**	C_p **Solid (kJ/kg K)**	C_p **Liquid (kJ/kg K)**	**Thermal Conductivity (W/m-K)**	**Dynamic Viscosity (kg/m-s)**	**Latent Heat of Fusion (kJ/kg)**
1%	1033.92	2758.09	2323.76	0.298	0.0079	180.006×10^3
5%	1137.61	2503.25	2124.46	0.335	0.0088	156.99×10^3
10%	1267.2	2243.35	1921.19	0.384	0.0101	133.517×10^3

4.11 Performance Indicators for the Melting of Nano-PCM

Percentage enhancement ratio (η) is a key performance indicator that quantitatively gauges melting enhancement at different time instances during the melting process. Equation (9) is used to calculate η which is plotted in **Figure: 4.15(a)** for all three concentrations of NEPCM with pure PCM Case-3 as the reference. All three cases show improved melting characteristics with the 10% NEPCM case showing the highest η. It is pertinent to mention that the η values for all the cases are greater than 10% at the 10 min mark which indicates faster melting during the initial stages. In contrast, the η values for all three Cases (pure PCM) are all less than 10% at the same time instant as was seen in **Figure: 4.1(a)**.

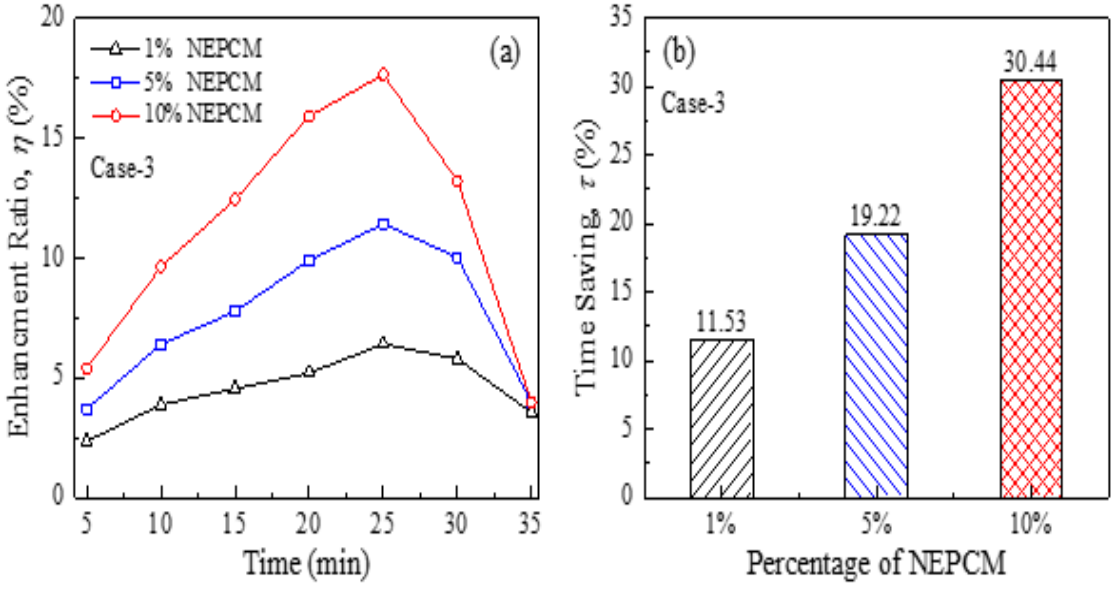

FIGURE 4.14: Comparison of the (a) Percentage Enhancement Ratio and (b) Percentage Time Saving for Various Concentrations of the NEPCM

In **Figure: 4.15(b)**, percentage time saving (τ) for all three concentrations of NEPCM is calculated and plotted. The τ values are seen to increase as the concentration of nanoparticles in the PCM increases. This trend is governed by the high enhancement ratio values for higher concentrations of the Nano-particles in the base phase change material.

4.12 Energy Storage and Storage Rate (Nano-PCM)

The addition of nanoparticles decreases the PCM content in the NEPCM. Energy is majorly stored by the PCM in the form of latent energy. Therefore, the addition of nanoparticles decreases the latent heat storage capacity of the NEPCM as suggested by Equation (9). This trend is visible in **Figure: 4.16(a)** where the total energy stored decreases with an increase in the nanoparticle concentration. The reference geometry (Case-3) with pure PCM is therefore, seen to accumulate the largest amount of energy. However, for cases with 5% and 10% NEPCM, this decrease is significant and must be considered while designing an LHTES system. A similar trend is also observed in the rates of energy storage as shown in **Figure: 4.16(b)**. Initially, the energy storage rates of the NEPCM cases are significantly higher compared to the reference case (Case-3, pure PCM). However, 10 minutes into the melting process, the energy storage rates become comparable to the reference case, eventually dipping below the benchmark with the exception of the case with 1% NEPCM, which remains comparable to the reference configuration.

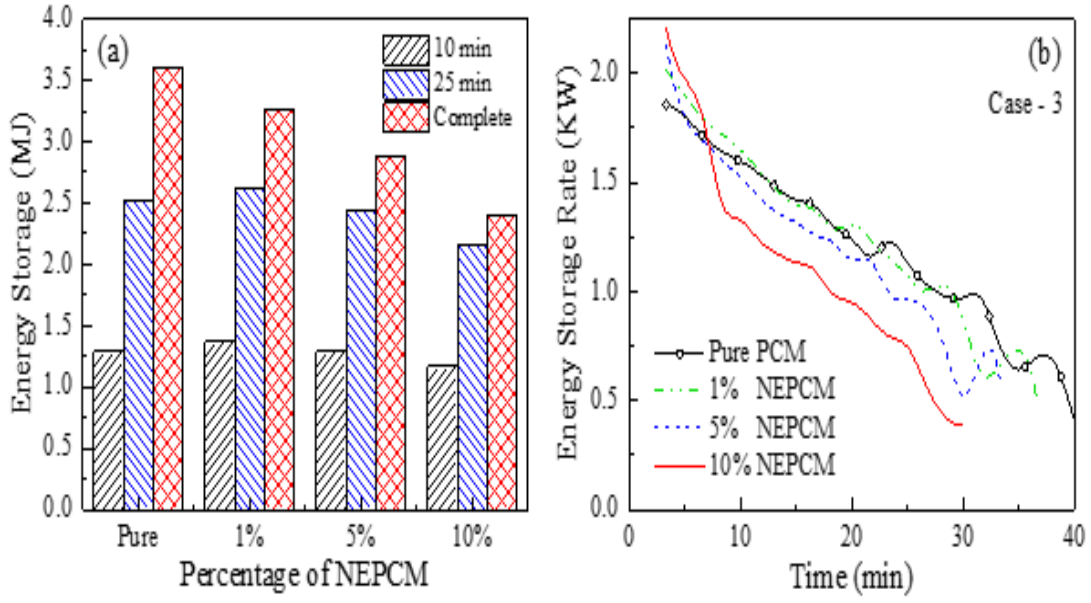

FIGURE 4.15: Comparison of (a) the Total Energy Stored in the NEPCM and (b) the Storage Rates for Various Concentrations of the NEPCM. Note that Case-3 with Pure PCM is Plotted as a Reference

4.13 Effects of Nano-Particles on Complete Melting-Solidification Cycle

The effects of adding Nano-particles in the PCM are studied for the double branched or leaf-vein patterned design, i.e., Case-3, which is the most efficient design for both the melting and solidification processes. Nano-particles are added in concentrations of 1%, 5% and 10% and the results are analyzed using different performance indicators by comparing against Case-3 with no Nano-particles.

The complete melting-solidification cycle of the PCM is simulated for all the cases. Case-3 with no Nano-particles completes the melting-solidification cycle in 263 minutes as shown in **Figure: 4.13 (a)**.

This is followed by the cases with 1%, 5% and 10% concentrations of Nano-particles which complete their melting-solidification cycle in 233 minutes, 208 minutes and 181 minutes, respectively. Higher is the concentration of Nano-particles quicker is the melting-solidification cycle completed.

It can be observed from the plots shown in **Figure: 4.13 (a)**. that the melting process is not much effected by the addition of Nano-particles, however, the solidification process is significantly accelerated.

This is due to the fact that the addition of Nano-particles enhances the thermal conductivity of the PCM, and since solidification is the conduction dominated phenomenon therefore it performs better as compared to the charging process which is mostly conquered through the convective heat transfer process.

As the concentration of the Nano-particles is increased above 10% there is not significant gain. This happen because a further increase in the Nano-particles volumetric concentration increases the density which increases the total melting-solidification cycle time [77]. Temporal variation of the average temperatures for all above mentioned cases is plotted in **Figure: 4.13 (b)**.

Case-3 with no Nano-particles attains minimum average temperature during melting among all the studied cases, whereas, all other cases with Nano-particles achieve almost same average temperatures above that value. Higher is the concentration of Nano-particles quicker is the melting-solidification cycle completed.

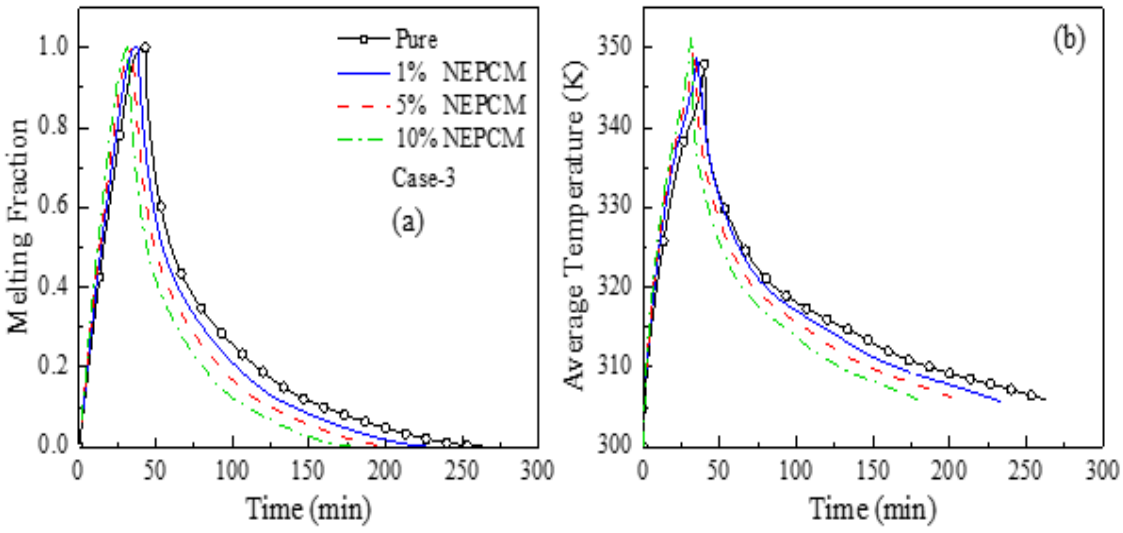

FIGURE 4.16: (a) Plots of Simultaneous Melting and Solidification Time Using Nano-Particles (B) Plots of Melting and Solidification Temperature for Nano-Particles

Percentage time saving 'τ' and the percentage enhancement ratio 'η' are used as performance indicators for the complete melting-solidification cycle of the PCM. These indicators are plotted for the Case-3 with Nano-particles added PCM as shown in **Figure: 4.14**. The reference is the Case-3 design with no Nano-particles.

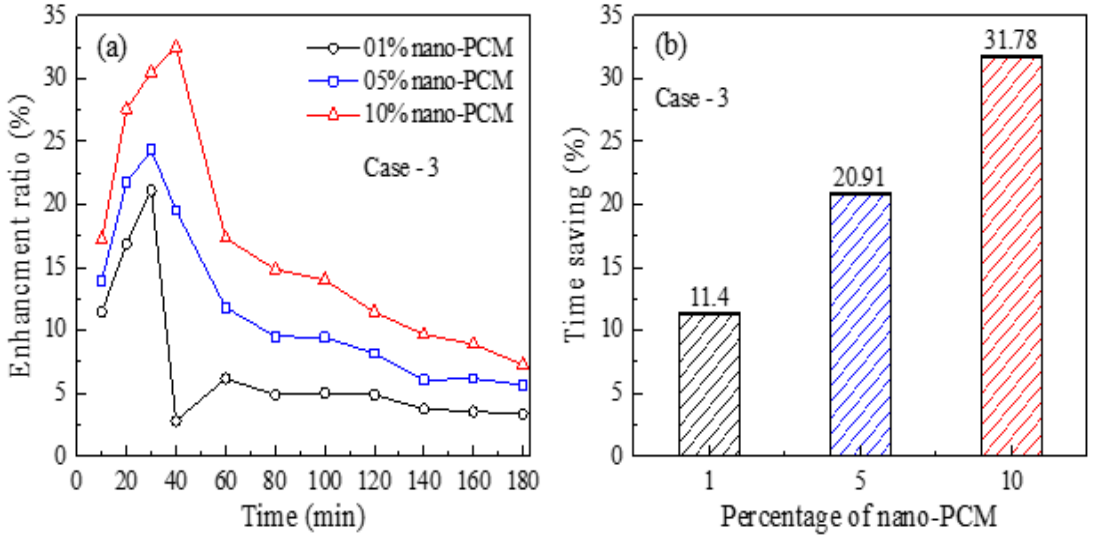

FIGURE 4.17: (a) Plots of Simultaneous Melting and Solidification Time Saving Using Nano-PCM (B) Plots of Enhancement Ratio of Simultaneous Melting and Solidification for Nano-PCM

The percentage time saving for the 1%, 5% and 10% Nano-particles concentrated PCM cases is 11.4%, 20.91% and 31.78%, respectively, as shown in **Figure: 4.14**

(a). Similarly, the percentage enhancement ratio plots shown in **Figure: 4.14 (b)** show spikes with a higher value for more Nano-particle concentration case. These enhancement peaks are observed at the start of the solidification process.

Chapter 5

Conclusion

A numerical study is performed to speed up the melting and solidification of PCM by enhancing the heat transfer between HTF and PCM in a horizontally installed shell and tube type latent heat thermal energy storage unit using effective fin designs and nano-particles. The simulation results of melting fraction of the Y-oriented triple-fin design base case reveal that a dump of solid PCM remain settled in the lower portion of the LHTES unit because a single fin directing downwards is not sufficient enough to effectively melt the whole PCM there. Based on this observation, five-fin designs are proposed out of which three fins are handling the lower half portion of the unit. Case-1 is an all-straight-fin design. In Case-2, three lower fins are single branched at the end. Case-3 comprises of lower three fins as double branched or leaf-vein patterned. All three cases, i.e., Case-1, Case-2 and Case-3, enhance the heat transfer process thereby accelerating the melting of PCM by a factor of 1.3, 1.55 and 1.85 as compared to the base case, respectively. Case-3 is therefore the best performing design. Contour plots of melting fraction, temperature and velocity are discussed to explain the convective currents generated in the molten PCM due to buoyancy effects. Percentage melting enhancement and percentage time saving are discussed as performance enhancement indicators for all three cases. Total melting time is saved by 22.9%, 35.4% and 45.9% respectively, as compared to the base case for three optimum cases. Heat storage rate and heat storage capacity of the new designs show that Case-3 stores more energy

as compared to the other two cases and also at a faster rate. The effects of HTF temperature are also explored on the melting time; higher the temperature of the HTF, faster is the melting.

The solidification process also suggests Case-3 as superior option but the gain is not as much as we got in the melting process. However, for the compete melting-solidification cycle, the Case-1, Case-2 and Case-3 shows time saving of 5.34%, 11.94% and 17.29%, respectively, as compared to the base case. The effects on nanoparticles on the melting-solidification cycle are analyzed by using different percentages of Al2O3 as nano-particles in the PCM for the Case-3 design. With 1%, 5% and 10% NEPCM, melting times are seen to reduce further by 11.5%, 19.2% and 26.9%, respectively, associated to optimum Case-3 by pure PCM. The addition of nanoparticles, however, decreases the latent heat of fusion of the NEPCM which consequently decreases the energy storage capacity and the storage rate as nanoparticles concentration is increased; a factor to be considered when designing an LHTES system. Total melting and solidification cycle using 10% volume concentration of nanoparticles saved 31.78% time as compared to the corresponding pure PCM case.

Bibliography

[1] M. R. Kadivar, M. A. Moghimi, P. Sapin, and C. N. Markides, "Annulus eccentricity optimisation of a phase-change material (PCM) horizontal double-pipe thermal energy store," *J. Energy Storage*, vol. 26, no. October, p. 101030, 2019.

[2] N. Belyakov, "Sustainable electricity management beyond generation," Sustain. *Power Gener.*, pp. 539–563, 2019.

[3] L. F. Cabeza, I. Martorell, L. Miró, A. I. Fernández, and C. Barreneche, Introduction to thermal energy storage (TES) systems. *Woodhead Publishing Limited*, 2015.

[4] Anon, "Applications of Thermal Energy Storage in the Cement Industry.," no. *September*, pp. 333–339, 2018.2.

[5] A. Sharma, V. V Tyagi, C. R. Chen, and D. Buddhi, "Review on thermal energy storage with phase change materials and applications," vol. 13, pp. 318–345, 2009.

[6] M. K. Rathod, "Thermal Stability of Phase Change Material."

[7] J. M. Khodadadi and S. F. Hosseinizadeh, "Nanoparticle-enhanced phase change materials (NEPCM) with great potential for improved thermal energy storage," Int. Commun. *Heat Mass Transf.*, vol. 34, no. 5, pp. 534–543, 2007, doi: 10.1016/j.icheatmasstransfer.2007.02.005.

[8] M. K. Rathod and J. Banerjee, "Thermal performance enhancement of shell and tube Latent Heat Storage Unit using longitudinal fins," *Appl. Therm. Eng.*, vol. 75, pp. 1084–1092, 2015, doi: 10.1016/j.applthermaleng.2014.10.074.

[9] I. Sarbu and A. Dorca, "Review on heat transfer analysis in thermal energy storage using latent heat storage systems and phase change materials," *Int. J. Energy Res.*, vol. 43, no. 1, pp. 29–64, 2019, doi: 10.1002/er.4196.

[10] L. Asip Khan and M. Mahabat Khan, "Role of orientation of fins in performance enhancement of a latent thermal energy storage unit," *Appl. Therm. Eng.*, vol. 175, no. April, p. 115408, 2020.

[11] F. Agyenim, N. Hewitt, P. Eames, and M. Smyth, "A review of materials, heat transfer and phase change problem formulation for latent heat thermal energy storage systems (LHTESS)," Renew. Sustain. *Energy Rev.*, vol. 14, no. 2, pp. 615–628, 2010, doi: 10.1016/j.rser.2009.10.015.

[12] A. A. Al-Abidi, S. Bin Mat, K. Sopian, M. Y. Sulaiman, C. H. Lim, and A. Th, "Review of thermal energy storage for air conditioning systems," *Renew. Sustain.* Energy Rev., vol. 16, no. 8, pp. 5802–5819, 2012, doi: 10.1016/j.rser.2012.05.030.

[13] M. Arıcı, F. Bilgin, S. Nižetić, and H. Karabay, "PCM integrated to external building walls: An optimization study on maximum activation of latent heat," *Appl. Therm. Eng.*, vol. 165, p. 114560, 2020, doi: 10.1016/j.applthermaleng.2019.114560.

[14] H. M. Ali and A. Arshad, "Experimental investigation of n-eicosane based circular pin-fin heat sinks for passive cooling of electronic devices," *Int. J. Heat Mass Transf.*, vol. 112, pp. 649–661, 2017.

[15] Q. Ren, P. Guo, and J. Zhu, "Thermal management of electronic devices using pin-fin based cascade microencapsulated PCM/expanded graphite composite," *Int. J. Heat Mass Transf.*, vol. 149, pp. 1–16, 2020, doi: 10.1016/j.ijheatmasstransfer.2019.119199.

[16] S. Bakhshipour, M. S. Valipour, and Y. Pahamli, "Analyse paramétrique de réfrigérateurs domestiques utilisant un échangeur de chaleur à matériau à changement de phase," *Int. J. Refrig.*, vol. 83, pp. 1–13, 2017, doi: 10.1016/j.ijrefrig.2017.07.014.

[17] M. A. Ezan, E. Ozcan Doganay, F. E. Yavuz, and I. H. Tavman, "A numerical study on the usage of phase change material (PCM) to prolong compressor off period in a beverage cooler," *Energy Convers. Manag.*, vol. 142, pp. 95–106, 2017, doi: 10.1016/j.enconman.2017.03.032.

[18] M. M. A. Khan, R. Saidur, and F. A. Al-Sulaiman, "A review for phase change materials (PCMs) in solar absorption refrigeration systems," Renew. *Sustain. Energy Rev.*, vol. 76, no. April 2016, pp. 105–137, 2017, doi: 10.1016/j.rser.2017.03.070.

[19] S. Seddegh, X. Wang, and A. D. Henderson, "A comparative study of thermal behaviour of a horizontal and vertical shell-and-tube energy storage using phase change materials," *Appl. Therm. Eng.*, vol. 93, pp. 348–358, 2016, doi: 10.1016/j.applthermaleng.2015.09.107.

[20] A. A. Al-Abidi, S. Mat, K. Sopian, M. Y. Sulaiman, and A. T. Mohammad, "Internal and external fin heat transfer enhancement technique for latent heat thermal energy storage in triplex tube heat exchangers," *Appl. Therm. Eng.*, vol. 53, no. 1, pp. 147–156, 2013, doi: 10.1016/j.applthermaleng.2013.01.011.

[21] A. A. Al-abidi, S. Mat, K. Sopian, M. Y. Sulaiman, and A. Th, "International Journal of Heat and Mass Transfer Numerical study of PCM solidification in a triplex tube heat exchanger with internal and external fins," *Int. J. Heat Mass Transf.*, vol. 61, pp. 684–695, 2013.

[22] A. M. Abdulateef, S. Mat, K. Sopian, J. Abdulateef, and A. A. Gitan, "Experimental and computational study of melting phase-change material in a triplex tube heat exchanger with longitudinal/triangular fins," *Sol. Energy*, vol. 155, pp. 142–153, 2017, doi: 10.1016/j.solener.2017.06.024.

[23] A. M. Abdulateef, S. Mat, J. Abdulateef, K. Sopian, and A. A. Al-Abidi, "Geometric and design parameters of fins employed for enhancing thermal energy storage systems: a review," *Renew. Sustain. Energy Rev.*, vol. 82, no. June 2016, pp. 1620–1635, 2018, doi: 10.1016/j.rser.2017.07.009.

[24] M. K. Saranprabhu and K. S. Rajan, "Magnesium oxide nanoparticles dispersed solar salt with improved solid phase thermal conductivity and specific heat for latent heat thermal energy storage," *Renew. Energy*, vol. 141, pp. 451–459, 2019, doi: 10.1016/j.renene.2019.04.027.

[25] R. P. Singh, H. Xu, S. C. Kaushik, D. Rakshit, and A. Romagnoli, "Effective utilization of natural convection via novel fin design & influence of enhanced viscosity due to carbon nano-particles in a solar cooling thermal storage system," *Sol. Energy*, vol. 183, no. February, pp. 105–119, 2019, doi: 10.1016/j.solener.2019.03.005.

[26] Z. Deng, X. Liu, C. Zhang, Y. Huang, and Y. Chen, "Melting behaviors of PCM in porous metal foam characterized by fractal geometry," *Int. J. Heat Mass Transf.*, vol. 113, pp. 1031–1042, 2017, doi: 10.1016/j.ijheatmasstransfer.2017.05.126.

[27] J. M. Mahdi and E. C. Nsofor, "Solidification enhancement in a triplex-tube latent heat energy storage system using nanoparticles-metal foam combination," *Energy*, vol. 126, pp. 501–512, 2017, doi: 10.1016/j.energy.2017.03.060.

[28] A. Kumar and S. K. Saha, "Latent heat thermal storage with variable porosity metal matrix: A numerical study," *Renew. Energy*, vol. 125, pp. 962–973, 2018, doi: 10.1016/j.renene.2018.03.030.

[29] E. B. S. Mettawee and G. M. R. Assassa, "Thermal conductivity enhancement in a latent heat storage system," *Sol. Energy*, vol. 81, no. 7, pp.

[30] F. Agyenim, P. Eames, and M. Smyth, "Heat transfer enhancement in medium temperature thermal energy storage system using a multitube heat transfer array," *Renew. Energy*, vol. 35, no. 1, pp.

[31] M. Esapour, M. J. Hosseini, A. A. Ranjbar, and R. Bahrampoury, "Numerical study on geometrical specifications and operational parameters of multi-tube heat storage systems," *Appl. Therm. Eng.*, vol. 109, pp. 351–363, 2016, doi: 10.1016/j.applthermaleng.2016.08.083.

[32] M. Esapour, M. J. Hosseini, A. A. Ranjbar, Y. Pahamli, and R. Bahrampoury, "Phase change in multi-tube heat exchangers," *Renew. Energy*, vol. 85, pp. 1017–1025, 2016, doi: 10.1016/j.renene.2015.07.063.

[33] J. Giro-Paloma, M. Martínez, L. F. Cabeza, and A. I. Fernández, "Types, methods, techniques, and applications for microencapsulated phase change materials (MPCM): A review," *Renew. Sustain. Energy Rev.*, vol. 53, pp. 1059–1075, 2016, doi: 10.1016/j.rser.2015.09.040.

[34] N. I. Ibrahim, F. A. Al-Sulaiman, S. Rahman, B. S. Yilbas, and A. Z. Sahin, "Heat transfer enhancement of phase change materials for thermal energy storage applications: A critical review," *Renew. Sustain. Energy Rev.*, vol. 74, no. October 2015, pp. 26–50, 2017.

[35] P. Henry, D. Groulx, F. Souayfane, and T. Chiu, "International Journal of Thermal Sciences In fl uence of fi n size and distribution on solid-liquid phase change in a rectangular enclosure," *Int. J. Therm. Sci.*, vol. 124, no. April 2017, pp. 433–446, 2018.

[36] A. Abhat, "Low temperature latent heat thermal energy storage: Heat storage materials," *Sol. Energy*, vol. 30, no. 4, pp. 313–332, 1983, doi: 10.1016/0038-092X(83)90186-X.

[37] J. M. Khodadadi and S. F. Hosseinizadeh, "Nanoparticle-enhanced phase change materials (NEPCM) with great potential for improved thermal energy storage," *Int. Commun. Heat Mass Transf.*, vol. 34, no. 5, pp. 534–543, 2007.

[38] J. Vogel and M. Johnson, "Natural convection during melting in vertical finned tube latent thermal energy storage systems," *Appl. Energy*, vol. 246, no. December 2018, pp. 38–52, 2019.

[39] J. C. Choi and S. D. Kim, "Heat-transfer characteristics of a latent heat storage system using MgCl2 · 6H2O," *Energy*, vol. 17, no. 12, pp. 1153–1164, 1992, doi: 10.1016/0360-5442(92)90004-J.

[40] M. J. Hosseini, A. A. Ranjbar, M. Rahimi, and R. Bahrampoury, "Experimental and numerical evaluation of longitudinally finned latent heat thermal storage systems," *Energy Build.*, vol. 99, pp. 263–272, 2015.

[41] B. Kamkari and D. Groulx, "Experimental investigation of melting behaviour of phase change material in finned rectangular enclosures under different inclination angles," *Exp. Therm. Fluid Sci.*, vol. 97, no. April, pp. 94–108, 2018.

[42] O. K. Yagci, M. Avci, and O. Aydin, "Melting and solidification of PCM in a tube-in-shell unit: Effect of fin edge lengths' ratio," *J. Energy Storage*, vol. 24, no. May, p. 100802, 2019.

[43] K. A. R. Ismail, C. L. F. Alves, and M. S. Modesto, "Numerical and experimental study on the solidifcation of PCM around a vertical axially finned isothermal cylinder," vol. 21, 2001.

[44] A. Castell, C. Solé, M. Medrano, J. Roca, L. F. Cabeza, and D. García, "Natural convection heat transfer coefficients in phase change material (PCM) modules with external vertical fins," *Appl. Therm. Eng.*, vol. 28, no. 13, pp. 1676–1686, 2008, doi: 10.1016/j.applthermaleng.2007.11.004.

[45] A. H. Mosaffa, F. Talati, H. Basirat Tabrizi, and M. A. Rosen, "Analytical modeling of PCM solidification in a shell and tube finned thermal storage for air conditioning systems," *Energy Build.*, vol. 49, pp. 356–361, 2012, doi: 10.1016/j.enbuild.2012.02.053.

[46] R. Velraj, R. V. Seeniraj, B. Hafner, C. Faber, and K. Schwarzer, "Experimental analysis and numerical modelling of inward solidification on a finned vertical tube for a latent heat storage unit," Sol. Energy, vol. 60, no. 5, pp. 281–290, 1997, doi: 10.1016/S0038-092X(96)00167-3.

[47] K. Ermis, A. Erek, and I. Dincer, "Heat transfer analysis of phase change process in a finned-tube thermal energy storage system using artificial neural network," *Int. J. Heat Mass Transf.*, vol. 50, no. 15–16, pp. 3163–3175, 2007, doi: 10.1016/j.ijheatmasstransfer.2006.12.017.

[48] S. Ebadi, S. H. Tasnim, A. A. Aliabadi, and S. Mahmud, "Melting of nano-PCM inside a cylindrical thermal energy storage system: Numerical study with experimental verification," *Energy Convers. Manag.*, vol. 166, no. January, pp. 241–259, 2018, doi: 10.1016/j.enconman.2018.04.016.

[49] A. Sciacovelli, F. Gagliardi, and V. Verda, "Maximization of performance of a PCM latent heat storage system with innovative fins," *Appl. Energy*, vol. 137, pp. 707–715, 2015, doi: 10.1016/j.apenergy.2014.07.015.

[50] M. K. Rathod and J. Banerjee, "Thermal performance enhancement of shell and tube Latent Heat Storage Unit using longitudinal fins," *Appl. Therm. Eng.*, vol. 75, pp. 1084–1092, 2015, doi: 10.1016/j.applthermaleng.2014.10.074.

[51] A. Sciacovelli, F. Gagliardi, and V. Verda, "Maximization of performance of a PCM latent heat storage system with innovative fins," *Appl. Energy*, vol. 137, pp. 707–715, 2015, doi: 10.1016/j.apenergy.2014.07.015.

[52] M. Eslami and M. A. Bahrami, "Sensible and latent thermal energy storage with constructal fins," *Int. J. Hydrogen Energy*, vol. 42, no. 28, pp. 17681–17691, 2017, doi: 10.1016/j.ijhydene.2017.04.097.

[53] K. T. Park, H. J. Kim, and D. K. Kim, "Experimental study of natural convection from vertical cylinders with branched fins," *Exp. Therm. Fluid Sci.*, vol. 54, pp. 29–37, 2014, doi: 10.1016/j.expthermflusci.2014.01.018.

[54] J. Xie, H. M. Lee, and J. Xiang, "Numerical study of thermally optimized metal structures in a Phase Change Material (PCM) enclosure," *Appl. Therm. Eng.*, vol. 148, no. August 2018, pp. 825–837, 2019.

[55] M. Sheikholeslami, A. N. Keshteli, and H. Babazadeh, "Nanoparticles favorable effects on performance of thermal storage units," *J. Mol. Liq.*, vol. 300, p. 112329, 2020, doi: 10.1016/j.molliq.2019.112329.

[56] M. Sheikholeslami, S. Lohrasbi, and D. D. Ganji, "Numerical analysis of discharging process acceleration in LHTESS by immersing innovative fin configuration using finite element method," *Appl. Therm. Eng.*, vol. 107, pp. 154–166, 2016, doi: 10.1016/j.applthermaleng.2016.06.158.

[57] A. Pizzolato, A. Sharma, K. Maute, A. Sciacovelli, and V. Verda, "Topology optimization for heat transfer enhancement in Latent Heat Thermal Energy Storage," *Int. J. Heat Mass Transf.*, vol. 113, pp. 875–888, 2017, doi: 10.1016/j.ijheatmasstransfer.2017.05.098.

[58] A. Pizzolato, A. Sharma, K. Maute, A. Sciacovelli, and V. Verda, "Design of effective fins for fast PCM melting and solidification in shell-and-tube latent heat thermal energy storage through topology optimization," *Appl. Energy*, vol. 208, no. September, pp. 210–227, 2017, doi: 10.1016/j.apenergy.2017.10.050.

[59] X. Luo and S. Liao, "Lattice Boltzmann simulation of tree-shaped fins enhanced melting heat transfer," *Numer. Heat Transf. Part A Appl.*, vol. 74, no. 5, pp. 1228–1243, 2018, doi: 10.1080/10407782.2018.1523598.

[60] J. Zheng, J. Wang, T. Chen, and Y. Yu, "Solidification performance of heat exchanger with tree-shaped fins," *Renew. Energy*, 2019, doi: 10.1016/j.renene.2019.1 0.091.

[61] M. Zhao, Y. Tian, M. Hu, F. Zhang, and M. Yang, "Topology optimization of fins for energy storage tank with phase change material," Numer. *Heat Transf. Part A Appl.*, vol. 0, no. 0, pp. 1–18, 2019, doi: 10.1080/10407782.2019.1690338.

[62] R. Elbahjaoui and H. El Qarnia, "Thermal analysis of nanoparticle-enhanced phase change material solidification in a rectangular latent heat storage unit

including natural convection," *Energy Build.*, vol. 153, pp. 1–17, 2017, doi: 10.1016/j.enbuild.2017.08.003.

[63] S. Liu, H. Peng, Z. Hu, X. Ling, and J. Huang, "Solidification performance of a latent heat storage unit with innovative longitudinal triangular fins," *Int. J. Heat Mass Transf.*, vol. 138, pp. 667–676, 2019, doi: 10.1016/j.ijheatmasstran sfer.2019. 04.121.

[64] J. M. Khodadadi and S. F. Hosseinizadeh, "Nanoparticle-enhanced phase change materials (NEPCM) with great potential for improved thermal energy storage," *Int. Commun. Heat Mass Transf.*, vol. 34, no. 5, pp. 534–543, 2007, doi: 10.1016/j.icheatmasstransfer.2007.02.005.

[65] S. A. Irfan, A. Shafie, N. Yahya, and N. Zainuddin, "Mathematical modeling and simulation of nanoparticle-assisted enhanced oil recovery - A review," *Energies*, vol. 12, no. 8, pp. 1–19, 2019, doi: 10.3390/en12081575.

[66] M. Parsazadeh and X. Duan, "Numerical study on the effects of fins and nanoparticles in a shell and tube phase change thermal energy storage unit," *Appl. Energy*, vol. 216, no. February, pp. 142–156, 2018, doi: 10.1016/j.apen ergy.2018.02 .052.

[67] S. Lohrasbi, S. Z. Miry, M. Gorji-Bandpy, and D. D. Ganji, "Performance enhancement of finned heat pipe assisted latent heat thermal energy storage system in the presence of nano-enhanced H2O as phase change material," *Int. J. Hydrogen Energy*, vol. 42, no. 10, pp. 6526–6546, 2017.

[68] J. M. Mahdi and E. C. Nsofor, "Solidification of a PCM with nanoparticles in triplex-tube thermal energy storage system," *Appl. Therm. Eng.*, vol. 108, pp. 596–604, 2016.

[69] S. Lohrasbi, M. G. Bandpy, and D. D. Ganji, "Response surface method optimization of V-shaped fin assisted latent heat thermal energy storage system during discharging process," *Alexandria Eng.* J., vol. 55, no. 3, pp. 2065–2076, 2016.

[70] A. A. Rabienataj Darzi, M. Jourabian, and M. Farhadi, "Melting and solidification of PCM enhanced by radial conductive fins and nanoparticles in cylindrical annulus," *Energy Convers. Manag.*, vol. 118, pp. 253–263, 2016, doi: 10.1016/j.enconman.2016.04.016.

[71] M. Alizadeh, Kh. Hossainzadeh, M.H. Shahvi and D.D.Ganji "Solidification acceleration in trplix tube heat exchanger using V-shape fins and nano-PCM," *Appl. Therm*, vol. 85, pp. 206–220, 2019, doi: 10.1016/j.applthermaleng.20 19.01 .073.

[72] M. Sheikholeslami, A. N. Keshteli, and A. Shafee, "Melting and solidification within an energy storage unit with triangular fin and CuO nano particles," *J. Energy Storage*, vol. 32, no. July, p. 101716, 2020, doi: 10.1016/j.est.2020.101 716.

[73] D. K. Singh, S. Suresh, H. Singh, B. A. J. Rose, S. Tassou, and N. Anantharaman, "Myo-inositol based nano-PCM for solar thermal energy storage," *Appl. Therm. Eng.*, vol. 110, pp. 564–572, 2017, doi: 10.1016/j.applthermaleng.2016. 08.202.

[74] A. M. Abdulateef, S. Mat, J. Abdulateef, K. Sopian, and A. A. Al-Abidi, "Thermal Performance Enhancement of Triplex Tube Latent Thermal Storage Using Fins-Nano-Phase Change Material Technique," *Heat Transf. Eng.*, vol. 39, no. 12, pp. 1067–1080, 2018, doi: 10.1080/01457632.2017.1358488.

[75] M. Arıcı, E. Tütüncü, Ç. Yıldız, and D. Li, "Enhancement of PCM melting rate via internal fin and nanoparticles," *Int. J. Heat Mass Transf.*, vol. 156, 2020, doi: 10.1016/j.ijheatmasstransfer.2020.119845.

[76] Y. Xuan and Q. Li, "Heat transfer enhancement of nanofluids," *Int. J. Heat Fluid Flow*, vol. 21, no. 1, pp. 58–64, 2000.

[77] T. Xiong, L. Zheng, and K. W. Shah, "Nano-enhanced phase change materials (NePCMs): A review of numerical simulations," *Appl. Therm. Eng.*, vol. 178, no. May, p. 115492, 2020, doi: 10.1016/j.applthermaleng.2020.115492.

[78] A. valan Arasu, A. P. Sasmito, and A. S. Mujumdar, "Numerical performance study of paraffin wax dispersed with alumina in a concentric pipe latent heat storage system," *Therm. Sci.*, vol. 17, no. 2, pp. 419–430, 2013, doi: 10.2298/TSCI110417004A.

[79] H. Babazadeh, M. A. Sheremet, H. A. Mohammed, M. R. Hajizadeh, and Z. Li, "Inclusion of nanoparticles in PCM for heat release unit," *J. Mol. Liq.*, vol. 313, 2020, doi: 10.1016/j.molliq.2020.113544.

[80] T. Van Hung, N. D. Nam, A. Zaib, and B. X. Vuong, "Nanomaterials for reduction of discharging time through a heat storage system," *J. Mol. Liq.*, vol. 312, p. 113396, 2020, doi: 10.1016/j.molliq.2020.113396.

[81] K. Hosseinzadeh, M. Alizadeh, and D. D. Ganji, "Solidification process of hybrid nano-enhanced phase change material in a LHTESS with tree-like branching fin in the presence of thermal radiation," *J. Mol. Liq.*, vol. 275, pp. 909–925, 2019, doi: 10.1016/j.molliq.2018.11.109.

[82] M. R. Hajizadeh, A. N. Keshteli, and Q. V. Bach, "Solidification of PCM within a tank with longitudinal-Y shape fins and CuO nanoparticle," *J. Mol. Liq.*, vol. 317, 2020, doi: 10.1016/j.molliq.2020.114188.

[83] F. Li et al., "Finned unit solidification with use of nanoparticles improved PCM," *J. Mol. Liq.*, vol. 314, 2020, doi: 10.1016/j.molliq.2020.113659.

[84] K. Hosseinzadeh, A. R. Mogharrebi, A. Asadi, M. Paikar, and D. D. Ganji, "Effect of fin and hybrid nano-particles on solid process in hexagonal triplex Latent Heat Thermal Energy Storage System," *J. Mol. Liq.*, vol. 300, p. 112347, 2020, doi: 10.1016/j.molliq.2019.112347.

[85] M. Sheikholeslami, "Numerical modeling of nano enhanced PCM solidification in an enclosure with metallic fin," *J. Mol. Liq.*, vol. 259, pp. 424–438, 2018, doi: 10.1016/j.molliq.2018.03.006.

[86] J. M. Mahdi and E. C. Nsofor, "Melting enhancement in triplex-tube latent thermal energy storage system using nanoparticles-fins combination," *Int. J.*

Heat Mass Transf., vol. 109, pp. 417–427, 2017, doi: 10.1016/j.ijheatmasstransfer.2017.02.016.

[87] A. D. Brent, V. R. Voller, and K. J. Reid, "Enthalpy-porosity technique for modeling convection-diffusion phase change: Application to the melting of a pure metal," *Numer. Heat Transf.*, vol. 13, no. 3, pp. 297–318, 1988, doi: 10.1080/10407788808913615.

[88] S. Deng, C. Nie, G. Wei, and W. B. Ye, "Improving the melting performance of a horizontal shell-tube latent-heat thermal energy storage unit using local enhanced finned tube," *Energy Build.*, vol. 183, pp. 161–173, 2019, doi: 10.1016/j.enbuild.2018.11.018.

[89] S. H. Tasnim, R. Hossain, S. Mahmud, and A. Dutta, "Convection effect on the melting process of nano-PCM inside porous enclosure," *Int. J. Heat Mass Transf.*, vol. 85, pp. 206–220, 2015, doi: 10.1016/j.ijheatmasstransfer.2015.01.073.